JOURNAL OF PETROLOGY | VOLUME 40 | NUMBER 6 | PAGES 1037–1064 | 1999

Effects of H_2O on Phase Relations during Crystallization of Gabbros in the Kap Edvard Holm Complex, East Greenland

MARK E. BRANDRISS[1]* AND DENNIS K. BIRD[2]

[1]DEPARTMENT OF GEOSCIENCES, WILLIAMS COLLEGE, 947 MAIN STREET, WILLIAMSTOWN, MA 01267, USA
[2]DEPARTMENT OF GEOLOGICAL AND ENVIRONMENTAL SCIENCES, STANFORD UNIVERSITY, STANFORD, CA 94305-2115, USA

RECEIVED JULY 15, 1998; REVISED TYPESCRIPT ACCEPTED JANUARY 8, 1999

In the Kap Edvard Holm Complex of East Greenland, layered olivine gabbros host numerous small, discordant bodies of ultramafic rock and magnetite gabbro that formed by late-magmatic metasomatic replacement of partially solidified gabbroic cumulates. Similar replacive rocks are also present as large semi-conformable sheet-like bodies within the layered gabbro sequence. Replacive bodies of all sizes are spatially associated with xenoliths of metabasaltic lava: the small bodies cluster around xenoliths, and the large bodies host swarms of xenoliths. The replacive bodies are inferred to have formed by reaction of gabbroic cumulates with pore liquids that were enriched in H_2O by degassing or dehydration melting of the metabasalts. As these liquids migrated through the cumulus pile, they resorbed plagioclase and produced ultramafic bodies. Where the liquids came to rest, they reacted with gabbroic cumulates to produce bodies of magnetite-rich gabbro. The most evolved pore liquids segregated to form hornblende-rich pegmatitic dikes of roughly dacitic composition, suggesting that hydration and possibly oxidation of the magma shifted the liquid line of descent from a tholeiitic trend toward a calc-alkaline trend. These inferences imply that contamination of magmas by dehydration of hydrothermally altered crustal rocks may significantly influence the evolution of mafic magma systems.

KEY WORDS: *gabbro; Kap Edvard Holm; metasomatism; postcumulus; xenolith*

INTRODUCTION

Studies of gabbroic and ultramafic intrusions have demonstrated that migration of reactive pore liquids commonly results in the formation of discordant igneous bodies within crystallizing cumulus sequences. In some cases, partially molten cumulates appear to have reacted with liquids or fluids that originated within the cumulus pile, resulting in resorption of cumulus minerals, crystallization of intrusive or replacive bodies, and redistribution of mass within the intrusion (e.g. Robins, 1982; Butcher, 1985; Butcher *et al.*, 1985; Helz, 1987; Irvine, 1987; Boudreau, 1988; McBirney & Sonnenthal, 1990; Larsen & Brooks, 1994; Scoon & Mitchell, 1994; Mathez, 1995; Meurer *et al.*, 1997; Boudreau, 1999). In other cases, partially molten cumulates are inferred to have reacted with externally derived magmas that intruded the cumulus pile, resulting in the development of discordant replacive bodies via the reaction of the cumulates with intruding magmas (e.g. Morse *et al.*, 1987; Bédard *et al.*, 1988; Tegner & Wilson, 1993; Tegner & Robins, 1996). Because cumulus rocks preserve records of magmatic fractionation and replenishment in large mafic intrusions, recognizing and understanding postcumulus processes such as these can provide insights into the evolution of mafic magma chambers and the differentiation of basaltic magmas within the crust.

Near the western margin of the Kap Edvard Holm Complex in East Greenland, layered gabbros host numerous small, discordant bodies of massive ultramafic and gabbroic rock that appear to have formed by late-magmatic replacement of partially solidified gabbroic cumulates. The same types of rock are also present as thick, semi-conformable layers within the layered gabbro sequence, where they appear to be largely replacive in

*Corresponding author. Telephone: (413) 458-2221. Fax: (413) 597-4116. E-mail: Mark.Brandriss@williams.edu

origin. The discordant bodies are spatially associated with xenoliths of metabasaltic lava derived from hydrothermally altered country rocks. On the basis of the field, petrographic, and geochemical evidence presented below, it is inferred that the discordant ultramafic and gabbroic bodies formed from magmas that were enriched in H_2O by degassing or dehydration melting of the metabasalts. This suggests that contamination of basaltic magmas by the water contained in hydrothermally altered crustal rocks may significantly influence the evolution of mafic magma systems.

GEOLOGIC SETTING

The Kap Edvard Holm Complex is an Eocene intrusive center in the Kangerdlugssuaq region of East Greenland (Fig. 1). It consists mainly of layered gabbros which are intruded locally by mafic dikes and syenitic plutons and breccias. The host rocks are Precambrian gneisses, Paleocene basaltic lavas, and volumetrically minor Cretaceous and early Tertiary sediments (Nielsen *et al.*, 1981; Kays *et al.*, 1989). Gabbros near the western margin of the complex contain abundant xenoliths of gneissic and metabasaltic country rock (Fig. 1; Brandriss *et al.*, 1996).

The layered gabbros have a stratigraphic thickness exceeding 5000 m, consisting mainly of plagioclase + augite ± olivine ± magnetite cumulates (Deer & Abbott, 1965; Wager & Brown, 1967; Elsdon, 1969, 1971*a*, 1971*b*; Abbott & Deer, 1972; Bernstein *et al.*, 1992, 1996; Tegner *et al.*, 1993). These cumulates crystallized from moderately evolved basaltic magmas in a chamber that was frequently replenished by fresh pulses of magma (Deer & Abbott, 1965; Bernstein *et al.*, 1992, 1996; Tegner *et al.*, 1993; Bird *et al.*, 1995).

The gabbro complex contains a small amount (<1%) of ultramafic rock, mostly of wehrlitic composition. At one locality, the layered gabbros are intruded by a discordant plug-like mass of wehrlite composed of anomalously magnesian minerals (Bernstein *et al.*, 1992, 1996). More typically, however, ultramafic rocks occur as sheets that are broadly conformable with the gabbro layering and consist of minerals having compositions nearly identical to those in the surrounding gabbros (Bernstein *et al.*, 1992, 1996; Tegner & Wilson, 1993; Arnason, 1995).

FIELD AND PETROGRAPHIC RELATIONSHIPS

The study area, located near the western margin of the complex, is a cluster of steep nunataks referred to collectively as 'Stand and Deliver Nunatak' (Fig. 2). The cliffs there expose ~250 m of layered gabbro section.

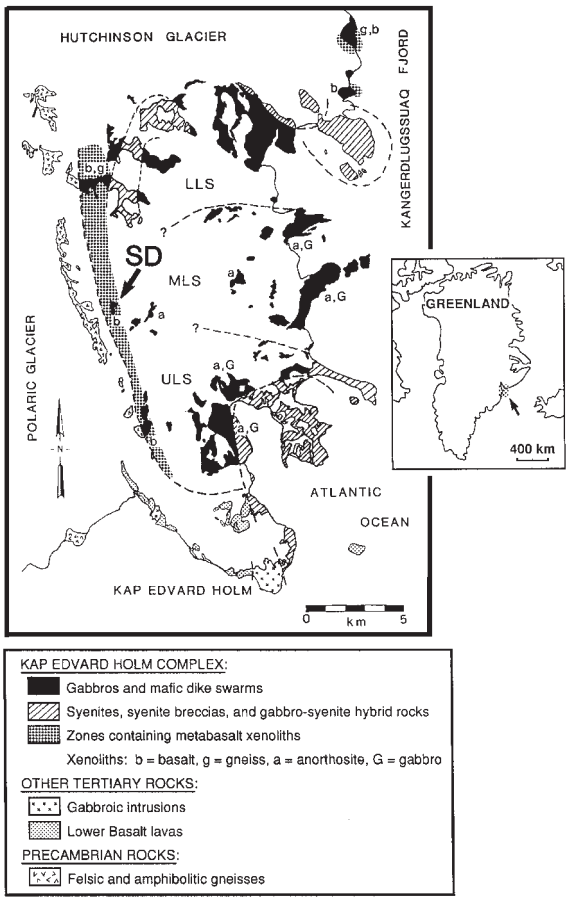

Fig. 1. Geologic map of the Kap Edvard Holm Complex, showing the location of the study area (SD, Stand and Deliver Nunatak) and the distribution of xenoliths in the gabbros. LLS, MLS and ULS are Lower, Middle and Upper Layered Series, respectively (after Elsdon, 1969).

Within the gabbros are abundant hornfelsed xenoliths of fine-grained metabasalt derived from country rock lavas that formed the upper walls and roof of the intrusion before exhumation [Brandriss *et al.*, 1996; the 'Lower Basalts' of Wager & Deer (1939), Nielsen *et al.* (1981) and Fram & Lesher (1997)]. The layered gabbros also host numerous semi-conformable to strongly discordant bodies of massive gabbro and ultramafic rock, ranging from centimeters to hundreds of meters in size.

Layered gabbros

Modally layered, laminated olivine gabbros constitute ~80% of the outcrop on Stand and Deliver Nunatak. In most of the area, layering is indistinct and consists only of faint centimeter- to meter-scale streaks or wisps of lighter or darker material (Fig. 3a), producing weakly layered rocks that will be referred to as 'ordinary' layered

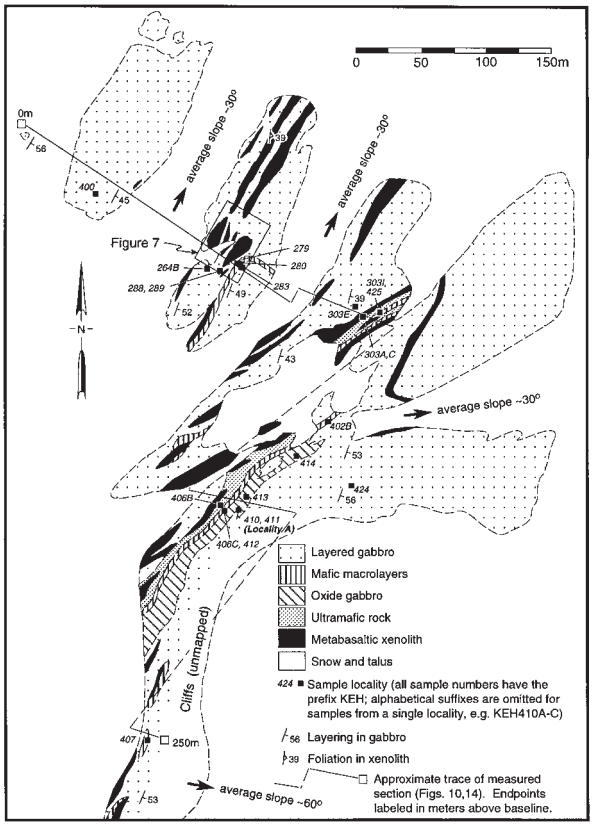

Fig. 2. Geologic map of Stand and Deliver Nunatak. The location is shown in Fig. 1.

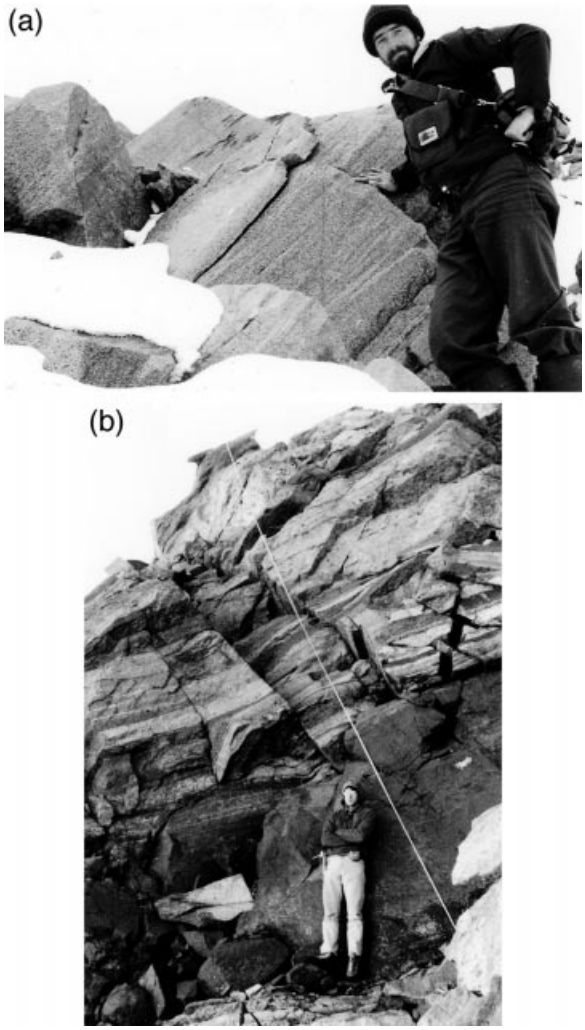

Fig. 3. (a) An outcrop of ordinary layered gabbro, showing the faint layering typical of gabbros through most of the section. (b) A zone of mafic macrolayering. The researcher is standing directly in front of an unusually large macrolayer, ~2·5 m thick; thinner layers are present in the upper half of the photo.

gabbros. Locally, however, the sequence contains prominent olivine-rich mafic layers that range from centimeters to meters in thickness and extend laterally for tens of meters or more. Such layering, which will be referred to as 'mafic macrolayering', is strongly developed in only a few narrow intervals within the section. Within these intervals, numerous closely spaced macrolayers are commonly present (Fig. 3b). The lower boundaries of mafic macrolayers are typically sharp; the upper boundaries may be sharp or gradational.

The layered gabbros are chiefly cumulates of plagioclase + augite + olivine (Fig. 4a). Magnetite is a minor granular phase throughout the upper half of the section but occurs more abundantly as intergranular crystals. Intergranular magnesiohornblende and orthopyroxene are commonly present in trace amounts (<0·1 vol. %), the orthopyroxene in some places replacing olivine along the margins of olivine grains. Plagioclase is commonly zoned, with normal zoning dominant and reverse zoning rare. The zoning is typically continuous, but embayed or anhedral cores are also common, suggesting a complex history of magma recharge and mixing (e.g. Davidson & Tepley, 1997).

The mafic macrolayers are mineralogically and texturally distinct from the ordinary layered gabbros. They are rich in olivine (up to 50 modal %, compared with 5–15% in the rest of the layered gabbros) and in some cases are notably rich in magnetite (Fig. 4b). Olivine is euhedral or rounded, with plagioclase and augite present mainly as subhedral or anhedral grains. Hornblende and phlogopite (~0·5 vol. %) are present as intergranular or ophitic crystals. The textures suggest that plagioclase and augite were lesser components of a cumulus assemblage dominated by olivine, with hydrous phases having grown from trapped pore liquids. Compositionally zoned plagioclase grains commonly have small anhedral or embayed cores, suggestive of episodes of plagioclase resorption followed by further growth.

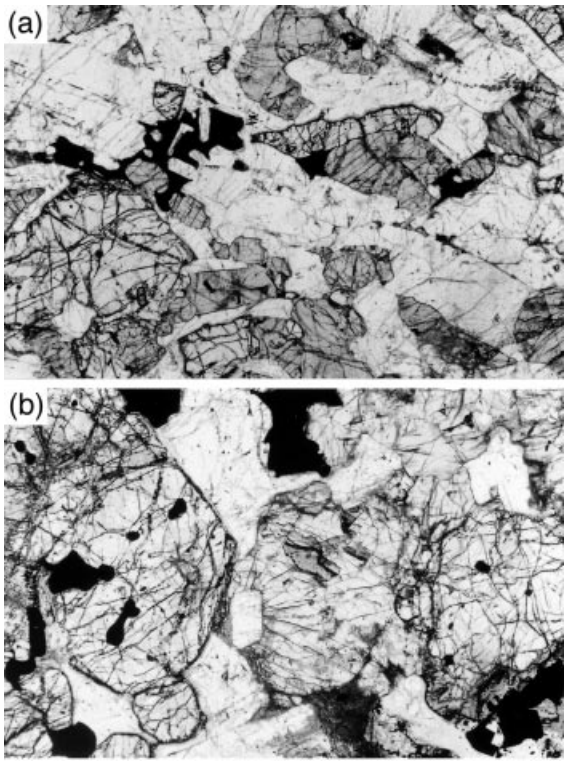

Fig. 4. (a) Ordinary layered gabbro (sample KEH264B). The field of view is 6 mm wide. Minerals are plagioclase, magnetite, olivine (high relief), and augite (gray). (b) Mafic macrolayer (sample KEH402B). A large grain of augite (center) surrounds a euhedral crystal of plagioclase and is flanked by two large grains of olivine. The field of view is 6 mm wide.

Macrolayers that are closely associated with ultramafic rocks (e.g. samples KEH412, KEH425) commonly have textures that are transitional from mafic macrolayer to ultramafic rock. These macrolayers contain cumulus plagioclase (like other mafic macrolayers) and mosaic aggregates of olivine crystals (like the ultramafic rocks described later).

Xenoliths

Fine-grained metabasaltic xenoliths, examined by Brandriss *et al.* (1996), make up roughly 10% of the outcrop. They tend to be concentrated in swarms, where they constitute up to 20% of outcrop over tens of meters of layered gabbro section. The xenoliths are lenticular or tabular, lie concordant to layering, and range from <1 m to >100 m in length, with the largest up to 5 m thick (Fig. 5).

The xenoliths are mainly granoblastic hornfelses of augite + plagioclase + magnetite ± orthopyroxene ± olivine ± ilmenite, from which various amounts of partial melt (<5% to 50% or more) have been extracted at temperatures ≥1050°C (Brandriss *et al.*, 1996). A few

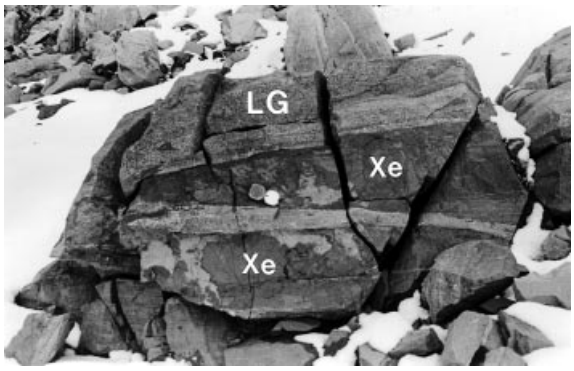

Fig. 5. Xenoliths of metabasalt (Xe) in layered gabbro (LG), with a Brunton compass for scale. These xenoliths are smaller than most, but the lenticular shapes are typical of xenoliths of all sizes.

xenoliths contain pegmatitic or gabbroic pods that crystallized from trapped partial melts. The pegmatitic pods contain abundant magnesiohornblende ± phlogopite, indicating that hydrous melts were produced from the xenoliths during anatexis. Low $\delta^{18}O$ values of the hornfelsic minerals (as low as –5·5‰ for pyroxene) indicate that the xenoliths were derived from protoliths that were altered by low-^{18}O meteoric–hydrothermal fluids before stoping (Brandriss *et al.*, 1996).

Ultramafic and oxide gabbro bodies

The layered gabbros at Stand and Deliver Nunatak host numerous massive, discordant bodies of ultramafic rock and magnetite-rich gabbro (the latter referred to hereafter as 'oxide gabbro'). The ultramafic and oxide gabbro bodies typically occur together and are conspicuously associated with xenoliths of metabasalt, suggesting that formation of the bodies was somehow related to stoping of the hydrothermally altered lavas that host the intrusion.

The ultramafic and oxide gabbro bodies comprise two distinct size populations. Small bodies, centimeters to meters in maximum dimension, occur as swarms of irregularly shaped pods or stringers that cut discordantly through the layered gabbros. Such bodies are typically found clustered within a meter or two of xenolith margins (e.g. Figs 6 and 7). Larger sheet-like bodies, typically hundreds of meters in extent, are found in two distinct stratigraphic intervals, where they form prominent units that are broadly concordant but locally transgressive to the gabbro layering. The large sheet-like ultramafic bodies commonly host abundant xenoliths of metabasalt.

Small ultramafic and oxide gabbro bodies

The small ultramafic bodies consist mainly of olivine, augite and orthopyroxene, with lesser magnetite and plagioclase, and minor amounts (≤2%) of hornblende,

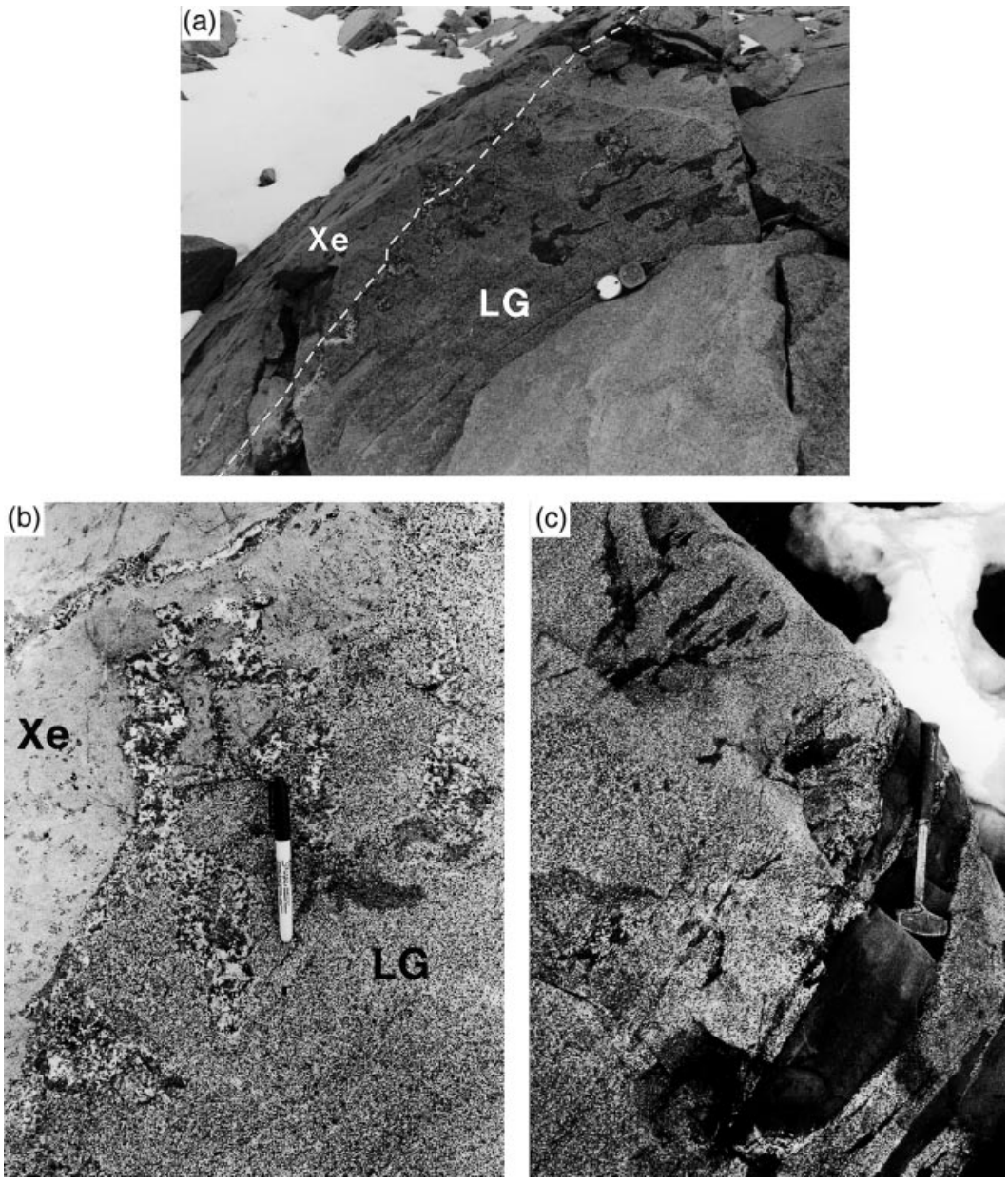

Fig. 6. (a) Ultramafic and oxide gabbro pods and stringers in layered gabbro (LG), immediately below a metabasaltic xenolith (Xe). The ultramafic pods are darker than the layered gabbro, and the oxide gabbro pods are lighter. Samples KEH288 and KEH289 are from right center. Brunton compass for scale. (b) Close-up of (a), showing oxide gabbro at the contact between layered gabbro (LG) and a mafic xenolith (Xe), with ultramafic bodies at right center. (c) A small metabasaltic xenolith with well-defined ultramafic bodies (center and upper left) and diffuse zones of coarse-grained (oxide?) gabbro.

phlogopite and apatite. Some bodies lie parallel or subparallel to layering in the host gabbros (e.g. Fig. 6a and c), but most are moderately to strongly discordant (Fig. 6b). The bodies invariably have sharp contacts with the layered gabbros. A few have complex branching forms that are preferentially deflected along planes of layering and lamination (Fig. 8), and some are discontinuously zoned from pyroxene-rich rims to olivine-rich cores (Fig. 8a).

Where pyroxene is the dominant mineral, the ultramafic rocks consist of granular augite, olivine, orthopyroxene, magnetite and apatite, with intergranular plagioclase, hornblende and phlogopite (Fig. 9a and b). Pyroxenes typically have ragged or consertal grain boundaries, unlike pyroxenes in the layered gabbros. The presence of abundant orthopyroxene (in some cases as abundant as augite) is noteworthy, as this mineral is present in the layered gabbros only as a trace inter-

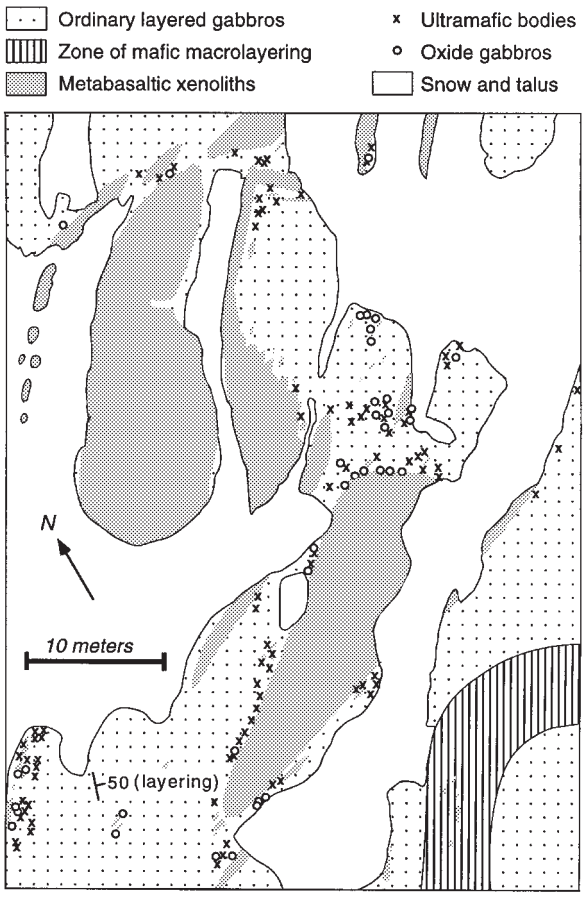

Fig. 7. Distribution of small-scale ultramafic and oxide gabbro bodies in a part of the study area. See Fig. 2 for location. The bodies (positions indicated schematically by × and ○ symbols) are typically the size of those shown in Fig. 6.

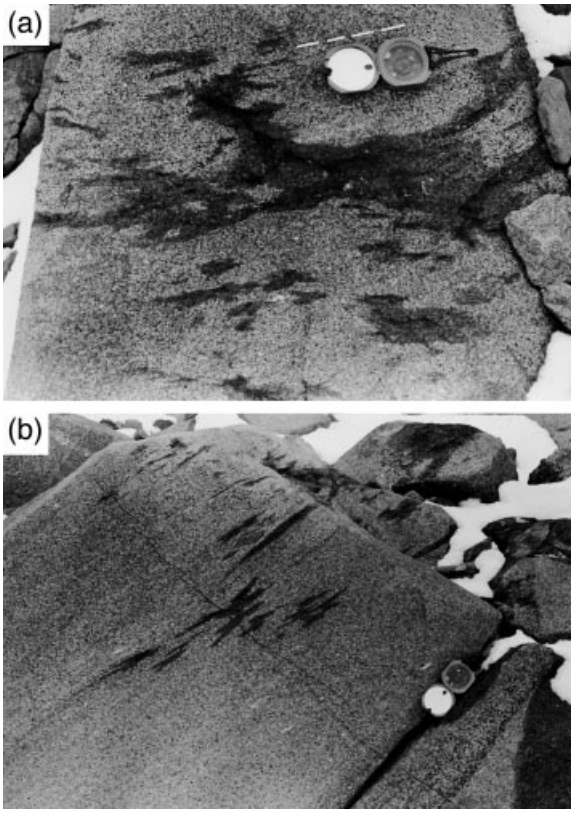

Fig. 8. (a) Branching ultramafic bodies, with preferential alignment along trend of gabbro layering (dashed line). Visible to the left of the compass is a zoned ultramafic body with a dark, deeply weathered olivine-rich core. (b) Outcrop surface perpendicular to the one shown in (a), showing ultramafic bodies lying in planes of layering and lamination.

granular phase. Orthopyroxene commonly has consertal grain boundaries against olivine, suggestive of a reaction relationship between the two minerals.

In rocks having olivine as the dominant mineral, the only granular phases are olivine and magnetite, with other minerals present as interstitial crystals (Fig. 9a). Thorough subsolidus alteration has destroyed most of the primary interstitial minerals, but augite, plagioclase, orthopyroxene and magnetite are identifiable.

The small oxide gabbro bodies consist of granular plagioclase, augite and magnetite, with minor intergranular hornblende and phlogopite (Fig. 9c). Olivine and orthopyroxene are conspicuously absent. The plagioclase in oxide gabbro bodies is euhedral to subhedral, whereas the augite and magnetite are subhedral to anhedral. This implies relatively early crystallization of plagioclase, in contrast to its late crystallization in the ultramafic bodies. The bodies have sharp to gradational contacts with the layered gabbros and typically occur as discordant pods or stringers, or, in a few places, as rinds along xenolith surfaces (Fig. 6a and b).

Large ultramafic and oxide gabbro bodies

Large ultramafic bodies, consisting of massive to faintly layered feldspathic peridotite, are found at the bases of mafic macrolayers in two stratigraphic intervals, as shown in Figs 2 and 10. The ultramafic bodies are sheet-like and broadly concordant to layering for tens of meters or more, and in most places they grade continuously upward into mafic macrolayers. Locally, however, the upper contacts of ultramafic bodies clearly crosscut the overlying layering, and the ultramafic rocks appear to replace the layered gabbros without obvious signs of deformation (Fig. 11a and b). Some ultramafic rocks contain faint layers that are locally continuous with layers in the adjacent gabbro, suggesting that the ultramafic rocks formed at least partly by *in situ* replacement of layered cumulates. This relationship is seen in Fig. 11.

The large ultramafic bodies are mineralogically and petrographically similar to the olivine-rich zones of small

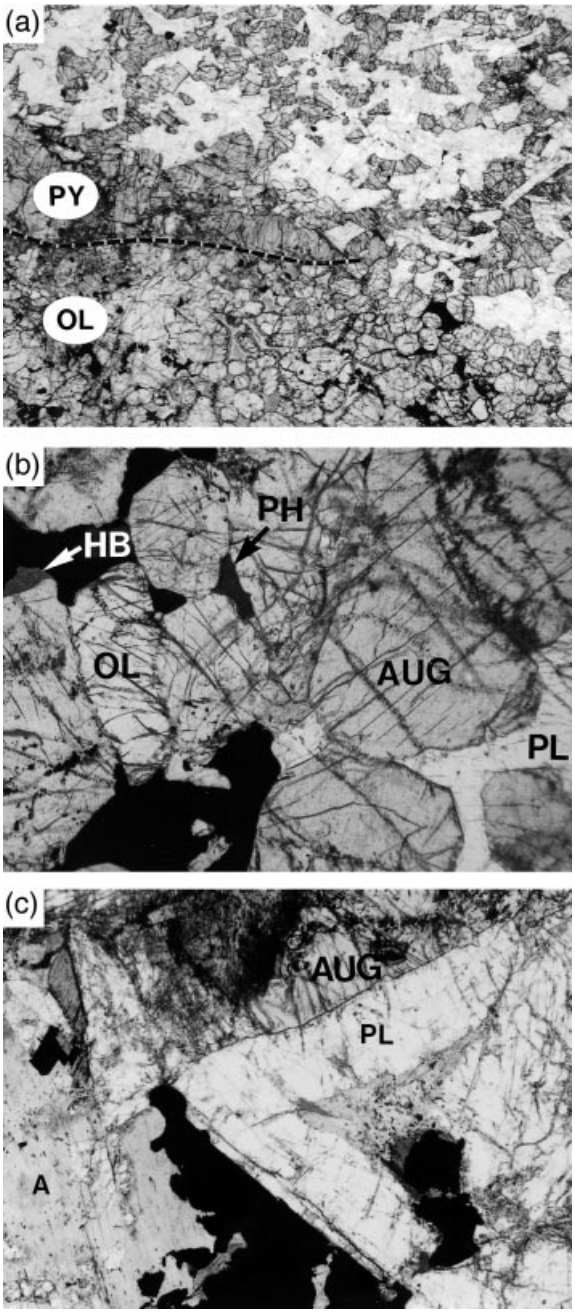

Fig. 9. (a) The contact between a small ultramafic body (bottom, sample KEH303H) and the surrounding layered gabbro (top). A wedge of pyroxene-rich rock (PY) separates an olivine-rich zone (OL) from the layered gabbro along part of the contact. The field of view is 25 mm wide. (b) Pyroxene-rich ultramafic body, sample KEH289. The field of view (3·5 mm wide) consists mostly of augite (AUG). Also present are magnetite, intergranular plagioclase (PL) and phlogopite (PH), a patch of brown hornblende (HB) replacing augite, and a single crystal of olivine (OL). Orthopyroxene is abundant in other parts of the thin section. (c) Typical small oxide gabbro body. PL, plagioclase; AUG, augite; A, secondary actinolite. The field of view is 6 mm wide.

ultramafic bodies described previously, except that in the large bodies, the interstitial minerals are better preserved. The large bodies contain granular olivine and magnetite, with augite, plagioclase, hornblende and phlogopite present as intergranular, ophitic or poikilitic crystals (Fig. 11c). Hornblende and phlogopite are conspicuously more abundant (1–2%) than in the layered gabbros. Olivine, magnetite and augite have euhedral faces against plagioclase, indicating that plagioclase formed late in the crystallization sequence.

A large body of oxide gabbro overlies one of the large bodies of ultramafic rock. This oxide gabbro is continuous for at least several hundred meters along strike (Fig. 2), and like the underlying ultramafic body, it is sheet-like and roughly conformable with the gabbro layering. The main part of the body is massive or weakly foliated, whereas the upper part is a complex transition zone in which oxide gabbro variably grades into, crosscuts, or intermingles with overlying layered gabbro. This transition zone is a patchwork of rock types including pegmatitic gabbro, fine-grained gabbro, contorted layered gabbro, and banded or wispy anorthosite. The lower boundary of the oxide gabbro body is not exposed, but it is presumably in contact with the mafic macrolayer or ultramafic body exposed a couple of meters downsection.

At one location where the upper contact of the oxide gabbro is fairly sharp, an apophysis of oxide gabbro penetrates the overlying layered gabbro (Locality A in Fig. 2), demonstrating that the oxide gabbro formed within an existing pile of layered gabbroic cumulates. A pegmatitic zone 30 cm wide is present along one contact of the apophysis, and the adjacent 'layered' olivine gabbro has a patchy, unlayered appearance (Fig. 12a). Along the other contact the layered olivine gabbro has recrystallized completely, forming pyroxene-rich and plagioclase-rich bands that are coplanar with the contact and oblique to the nearby layering. Olivine has disappeared from the layered gabbro within tens of centimeters of this second contact, and the abundance of magnetite is far greater than in ordinary layered gabbro, suggesting that oxide gabbro locally formed by replacement of layered olivine gabbro.

The large oxide gabbro body is mineralogically and texturally similar to the small oxide gabbro bodies described above, with magnetite and hornblende being anomalously abundant (up to ~10% and 1%, respectively) and olivine being conspicuously absent (Fig. 12b). Most of the hornblende formed relatively late, at the expense of augite or as an intergranular mineral.

Hornblende–andesine pegmatite dikes

The large oxide gabbro and ultramafic bodies are cut by leucocratic pegmatite dikes consisting of

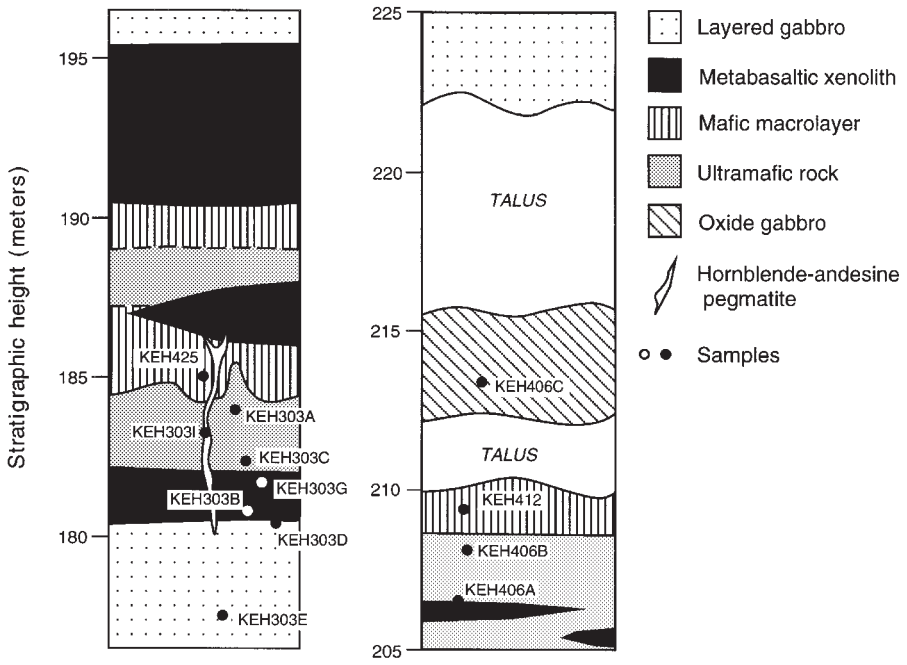

Fig. 10. Sections through two stratigraphic intervals containing large sheet-like ultramafic bodies. The localities of samples analyzed in this study and by Brandriss *et al.* (1996) are indicated. Locations of the sections are shown by the sample numbers in Fig. 2.

andesine + hornblende + apatite + Fe–Ti oxides ± augite ± phlogopite (Fig. 13). These dikes are volumetrically minor, constituting ≪1% of the outcrop areas of oxide gabbro and ultramafic rock. The pegmatites fill elongate gashes, centimeters thick and up to several meters long, and have the appearance of late-stage liquid segregations that filled fractures in nearly solidified cumulates. One such dike was found in a mafic macrolayer, but none have been found in ordinary layered gabbro.

Secondary alteration

All of the rocks contain secondary hydrothermal minerals (Brandriss *et al.*, 1995). The most common assemblage is actinolite, chlorite, talc, magnetite, and orthoamphibole, similar to the actinolitic hornblende + chlorite + talc alteration type described by Bird *et al.* (1988). A less common assemblage, found mainly in the oxide gabbros and hornblende–andesine pegmatites, contains epidote, albite, actinolite, chlorite, sericite, titanite, hedenbergite, and minor hornblende, equivalent to the calcic amphibole + epidote + albite assemblage of Bird *et al.* (1988). The oxide gabbros and hornblende–andesine pegmatites are the most altered rocks, typically containing 20–80% secondary minerals, whereas other rock types typically contain only 1–10% secondary minerals. Low values of δD and $\delta^{18}O$ indicate that the secondary minerals formed from hydrothermal fluids of meteoric origin (Fehlhaber & Bird, 1991; Nevle *et al.*, 1994; Brandriss *et al.*, 1995).

GEOCHEMISTRY

Mineral compositions

Representative electron microprobe analyses of minerals in the gabbroic, ultramafic and pegmatitic rocks are presented in Tables 1–3 and summarized in Fig. 14. Analyses of minerals in xenoliths have been reported by Brandriss *et al.* (1996), and a complete tabulation of analyses has been given by Brandriss (1993).

Augite and olivine have narrow compositional ranges, with differences among rock types limited to a few mole percent of any major component. Augite compositions vary between $Wo_{41}En_{46}Fs_{13}$ and $Wo_{42}En_{43}Fs_{15}$ (Table 1, Fig. 14) and olivine compositions vary between Fo_{70} and Fo_{74} (Table 2, Fig. 14). There is a weak tendency for the mafic silicates to be slightly more magnesian in the melanocratic rocks and slightly less magnesian in the oxide gabbros (Fig. 14), and a strong tendency for the augite in oxide gabbros to be impoverished in Cr relative to the augite in other rocks (Table 1). Among the layered gabbros, there are no regular compositional variations with height in the stratigraphic section, as shown in Fig. 14.

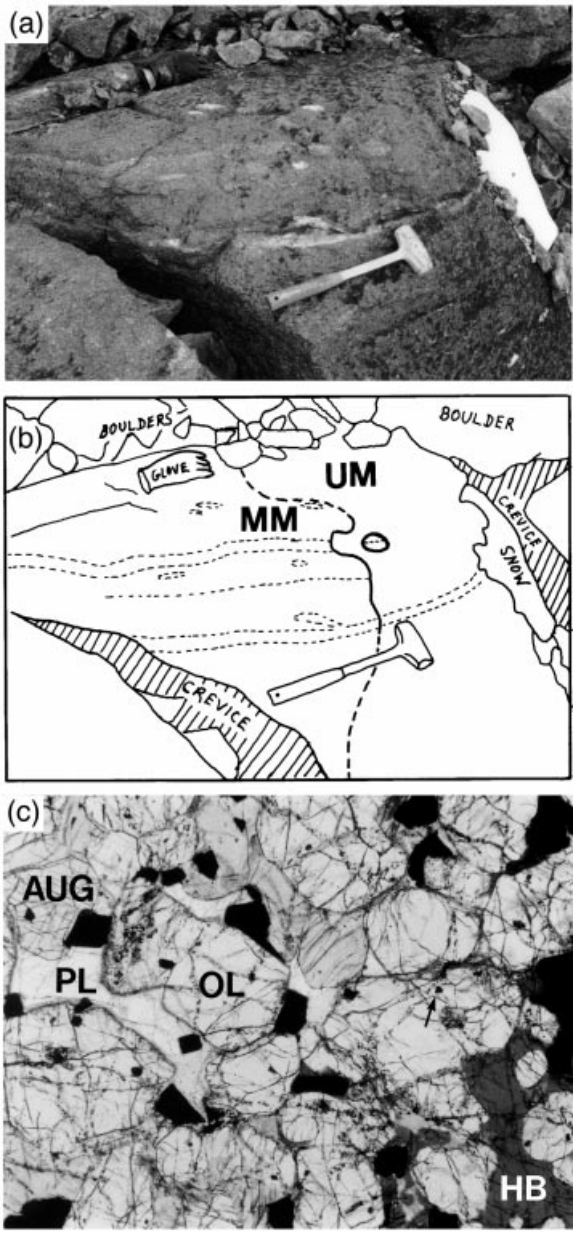

Fig. 11. (a) Mafic macrolayer (left) and discordant apophysis from underlying large sheet-like ultramafic body (right). This outcrop is near the site of samples KEH303A and KEH425. (b) Drawing of (a). The contact is shown by the line separating a mafic macrolayer (MM) from massive ultramafic rock (UM). The prominent leucocratic layer immediately above the hammer can be traced into the ultramafic body, but the less distinct layers above it have been truncated. (c) Thin section of large ultramafic body (sample KEH406B). Granular olivine (OL), containing euhedral chadacrysts of magnetite (e.g. minute crystal at arrow), is enclosed in intergranular to poikilitic augite (AUG), magnetite, plagioclase (PL) and hornblende (HB). The field of view is 6 mm wide.

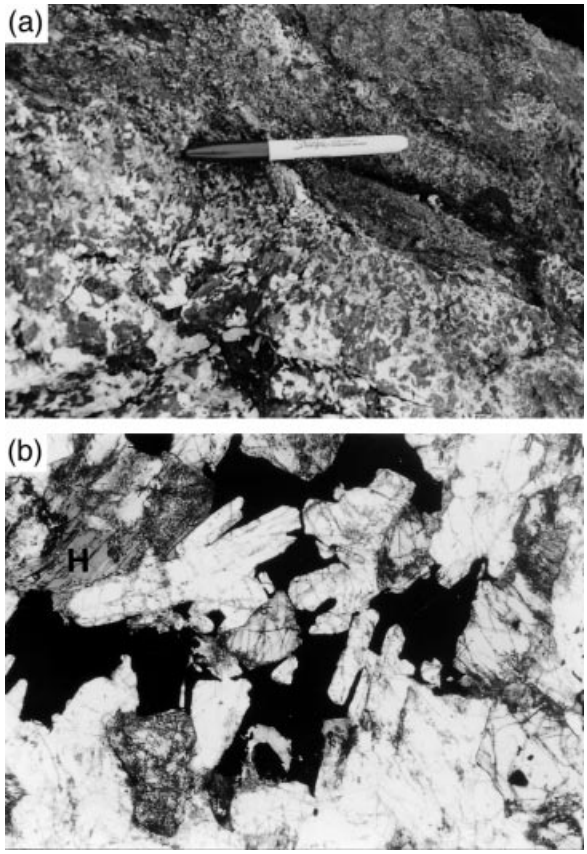

Fig. 12. (a) Contact between pegmatitic oxide gabbro (at lower left) and 'layered' gabbro (at upper right), from margin of discordant apophysis of oxide gabbro that penetrates overlying layered gabbro (Locality A in Fig. 2). Layering has been obliterated near the contact. (b) Typical oxide gabbro (sample KEH406C), consisting of plagioclase (white), augite (pale gray), magnetite (black), and intergranular hornblende (H, near upper left). The field of view is 6 mm wide.

Plagioclase is compositionally more variable than the mafic silicates, with compositions dependent on rock type and on the textural character of the grains. Selected electron microprobe analyses are presented in Table 3, and the relationships between composition and texture are shown in Fig. 14. In samples of ordinary layered gabbro, the composition of cumulus plagioclase (homogeneous grains, or the cores of regularly zoned grains) ranges from An_{60} to An_{68} (Fig. 14). Plagioclase in the mafic macrolayers overlaps this range but extends to more calcic compositions (Fig. 14). The highest recorded anorthite content (An_{78}) was measured in the embayed core of a zoned grain in a mafic macrolayer (sample KEH280, Table 3). Like the compositions of the mafic silicates, the composition of plagioclase in the layered rocks does not vary systematically with height in the stratigraphic section (Fig. 14).

Plagioclase in the oxide gabbros overlaps the compositional range in ordinary layered gabbros but extends to slightly more sodic compositions ($An_{54–68}$, excluding rims of zoned crystals). The rims of zoned grains in all varieties of gabbro tend to be relatively sodic (typically An_{55} to An_{60}), as do the poikilitic and intergranular

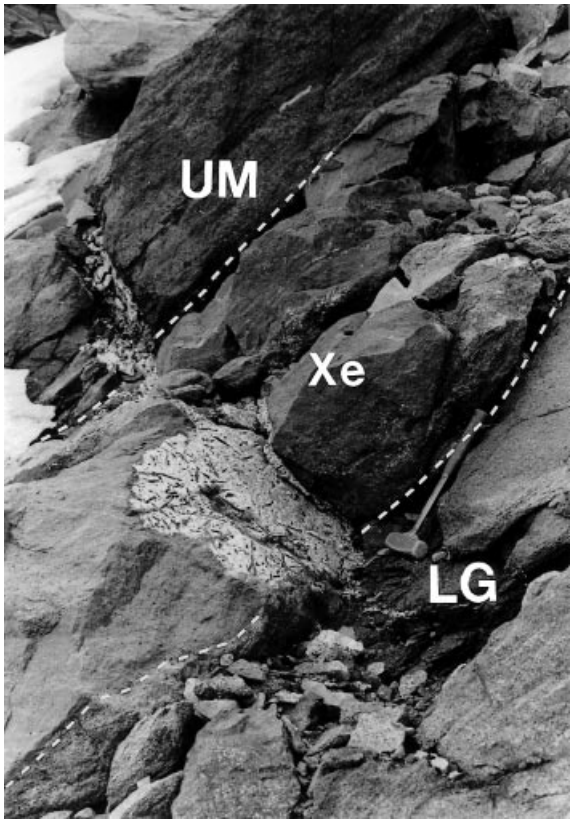

Fig. 13. Hornblende–andesine pegmatite dike (sample KEH303I) cutting faintly layered ultramafic rock (UM) and a metabasaltic xenolith (Xe) before pinching out in layered gabbro (LG).

crystals in ultramafic bodies (typically An_{57} to An_{59} but as low as An_{28}). In the hornblende–andesine pegmatite dikes, measured plagioclase compositions range from An_{28} to An_{43} (Table 3), consistent with the interpretation that the dikes crystallized from segregations of late-stage, highly evolved pore liquids.

Primary hornblende in the ultramafic and oxide gabbro bodies and pegmatitic dikes is of magnesiohornblende composition, with atomic Mg/(Mg + Fe) ranging from 0·70 to 0·77. There are no systematic differences among the various rock types. Representative analyses have been presented by Brandriss *et al.* (1995) and a complete tabulation has been given by Brandriss (1993). It must be noted that as a result of typographical errors in table 2 of Brandriss *et al.* (1995), samples KEH303I and KEH402A were listed incorrectly as xenoliths, whereas they are actually dikes of hornblende–andesine pegmatite.

Mineral thermometry

Brandriss (1993) used the compositions of augites and orthopyroxenes in the small ultramafic bodies to calculate crystallization temperatures using the two-pyroxene geothermometer of Davidson & Lindsley (1989) in the form presented by Lindsley & Frost (1992) and Andersen *et al.* (1993). Calculated temperatures ranged from approximately 1020°C to 1070°C. Assuming uncertainties of about ±30°C (Frost & Lindsley, 1992), this defines a temperature range of ~990–1100°C, implying crystallization under magmatic conditions.

Whole-rock compositions

Major and trace element compositions of representative whole-rock samples have been determined by X-ray fluorescence (XRF) analysis. Data for a few samples have been supplemented by instrumental neutron activation analysis (INAA) of rare earth elements (REE) and additional trace elements. Results are presented in Table 4 and summarized graphically in Figs 15 and 16.

In Fig. 15, the compositions of ultramafic rocks and oxide gabbros are compared with the compositions of ordinary layered gabbros. Relative to the ordinary layered gabbros, the ultramafic rocks are rich in the constituents of mafic minerals (Mg, Fe, Mn, Ti, Cr, V, Ni, Nb) and poor in the constituents of feldspar (Ca, Na, K, Al, Sr). The oxide gabbros have relatively high abundances of elements normally concentrated in Fe–Ti spinel phases (Fe, Ti, V, Nb) and have higher ratios of Fe/Mg, consistent with the anomalously high abundance of magnetite. Interestingly, however, the oxide gabbros are impoverished in Cr relative to other rock types, despite the tendency of Cr to partition strongly into magnetite. Not shown in Fig. 15 is the composition of a pegmatitic dike (Table 4), which is exceptionally rich in incompatible elements (e.g. Rb, Ba, Zr, Nb, P, K, Y, Th, REE) and poor in compatible elements (e.g. Cr, Ni).

Chondrite-normalized REE patterns for rocks analyzed by INAA are presented in Fig. 16. The layered gabbro has a positive Eu anomaly that obviously reflects the accumulation of plagioclase. The ultramafic rock and hornblende–andesine pegmatite have negative Eu anomalies, suggesting that they formed from magmas that had fractionated plagioclase previously. This is a surprising inference for the ultramafic rock, which contains plagioclase only as a late intergranular phase. It is less surprising for the hornblende–andesine pegmatite dike, in which the negative Eu anomaly, high La/Yb, and high concentrations of REE and other incompatible elements are consistent with formation of the dike by late-stage segregation of evolved pore liquid.

Strontium isotopes

Strontium isotope analyses of six plutonic and xenolithic samples are presented in Table 5. Calculated initial

Table 1: Representative electron microprobe analyses of augite, and range of compositions in each sample

	Layered gabbros											
	Ordinary layered gabbros						Adjacent to small ultramafic body		Mafic macrolayers			
Sample:*	264B	279	282	303E	400	424	289	303H	280	402B	412	425
Analysis no:	13	50-2	51	50	9	14	22	10	50-1	58	10	15
SiO_2	51·73	50·61	51·03	50·67	51·23	51·00	51·55	51·00	51·04	50·84	51·86	52·12
Al_2O_3	3·01	3·39	2·78	3·01	3·07	3·77	3·17	3·03	2·48	2·75	2·88	2·90
FeO	8·46	8·77	8·74	8·76	7·90	8·49	8·49	8·91	8·88	8·83	7·84	8·26
MnO	0·04	0·15	0·28	0·33	0·26	0·27	0·21	0·25	0·16	0·25	0·15	0·31
MgO	15·40	15·84	15·47	15·04	15·14	14·94	15·26	14·97	15·94	15·61	15·52	15·81
CaO	20·93	20·43	20·73	21·27	21·33	20·27	20·36	19·87	19·98	20·47	19·98	19·90
Na_2O	0·36	0·37	0·38	0·35	0·33	0·42	0·37	0·38	0·36	0·37	0·39	0·41
TiO_2	0·92	1·13	1·06	1·04	0·99	1·25	1·13	1·08	1·10	1·13	1·02	1·20
Cr_2O_3	0·12	0·17	0·37	0·17	0·08	0·28	0·12	0·26	0·21	0·09	0·29	0·28
Total	100·97	100·84	100·84	100·63	100·33	100·69	100·66	99·75	100·15	100·32	99·93	101·19
Wo	42·7	41·4	42·2	43·4	43·9	42·5	42·2	41·7	40·7	41·7	41·9	41·2
En	43·8	44·7	43·9	42·7	43·4	43·6	44·0	43·7	45·2	44·3	45·3	45·5
Fs	13·5	13·9	13·9	13·9	12·7	13·9	13·7	14·6	14·1	14·0	12·8	13·3
Mg/(Mg + Fe)	0·764	0·763	0·759	0·754	0·774	0·758	0·762	0·750	0·762	0·759	0·779	0·773
Range: low	0·760	0·752	0·758	0·750	0·769	0·752	0·754	0·750	0·753	0·730	0·774	0·768
high	0·771	0·763	0·764	0·756	0·783	0·769	0·762	0·762	0·762	0·762	0·779	0·800
No. of analyses	3	2	3	3	3	3	2	2	3	3	2	3

Table 1: continued

	Ultramafic bodies					Oxide gabbro bodies							
	Large sheets			Small bodies		Large sheet							Small body
Sample:*	303A	303C	406B	289	303H	406C	411	410A	410B	410C	413	414	288
Analysis no:	6	8	53	19	11	3	56-2	3	2	1	2	54	55
SiO_2	50·47	50·52	51·18	51·42	50·93	51·35	50·48	51·82	52·80	51·70	50·75	50·10	51·95
Al_2O_3	2·65	2·94	2·94	2·92	2·94	2·98	2·97	3·01	1·71	2·77	2·99	3·24	1·72
FeO	8·21	8·00	9·18	8·45	8·56	8·88	9·33	9·04	8·54	8·89	9·04	9·28	8·46
MnO	0·07	0·04	0·25	0·20	0·26	0·00	0·18	0·19	0·14	0·23	0·20	0·20	0·13
MgO	15·25	15·65	15·96	15·33	14·84	15·03	15·00	15·00	15·17	15·29	15·32	15·10	15·96
CaO	20·15	19·72	19·88	20·02	20·19	20·67	20·76	20·57	21·23	20·82	20·90	20·93	21·27
Na_2O	0·36	0·36	0·40	0·36	0·34	0·34	0·29	0·35	0·34	0·37	0·36	0·36	0·37
TiO_2	0·99	1·09	0·98	1·03	1·05	1·15	1·04	1·13	0·64	1·06	1·19	1·14	0·68
Cr_2O_3	0·14	0·10	0·15	0·23	0·13	0·02	0·01	0·01	0·01	0·08	0·02	0·04	0·04
Total	98·29	98·42	100·92	99·96	99·24	100·42	100·05	101·12	100·58	101·21	100·77	100·37	100·58
Wo	42·2	41·3	40·4	41·8	42·5	42·6	42·4	42·4	43·3	42·5	42·4	42·6	42·5
En	44·4	45·6	45·1	44·5	43·5	43·1	42·7	43·0	43·1	43·4	43·3	42·7	44·4
Fs	13·4	13·1	14·5	13·8	14·1	14·3	14·9	14·5	13·6	14·2	14·3	14·7	13·2
Mg/(Mg+Fe)	0·768	0·777	0·756	0·764	0·756	0·751	0·741	0·747	0·760	0·754	0·751	0·744	0·771
Range: low			0·756	0·758	0·755	0·748	0·741	0·746	0·760	0·754	0·748	0·743	0·767
high			0·769	0·784	0·756	0·755	0·752	0·748	0·761	0·756	0·751	0·757	0·771
No. of analyses	1	1	2	5	2	3	3	3	2	2	2	3	2

* All sample numbers have the prefix KEH.
Analyses were made by wavelength-dispersive electron microprobe analysis at Stanford University and the University of California, Davis. Silicate minerals and metal oxides were used as calibration standards. Details of analytical procedures have been given by Brandriss (1993).

Table 2: Representative electron microprobe analyses of olivine, and range of compositions in each sample

	Layered gabbros											Ultramafic bodies				
	Ordinary layered gabbros						Adjacent to small ultramafic body		Mafic macrolayers			Large sheets			Small bodies	
Sample:*	264B	279	282	303E	400	424	289	303H	280	402B	425	303A	303C	406B	289	303H
Analysis no.:	10	55	56	54	5	12	11	6	57	53	10	5	11	6	10	4
SiO_2	38·36	36·51	36·98	37·19	38·18	37·41	38·72	38·09	37·18	36·91	38·62	37·54	38·53	38·20	38·63	37·99
MgO†	36·35	35·57	36·07	35·65	35·90	35·46	37·49	36·55	35·62	35·14	37·66	36·63	37·69	36·13	37·78	36·71
FeO†	26·24	27·73	27·79	27·89	26·38	27·48	24·85	26·25	27·56	28·35	24·71	25·20	24·66	26·15	24·43	26·42
CaO	n.a.	0·09	0·02	0·13	n.a.	n.a.	n.a.	n.a.	0·12	0·09	n.a.	n.a.	n.a.	n.a.	n.a.	n.a.
MnO	0·43	0·28	0·42	0·42	0·52	0·34	0·39	0·41	0·65	0·52	0·43	0·46	0·28	0·32	0·46	0·39
Total	101·38	100·18	101·28	101·3	100·98	100·69	101·45	101·30	101·13	101·01	101·42	99·83	101·16	100·80	101·30	101·51
Fo†	71·2	*71·1*	*71·3*	*71·0*	70·8	69·7	72·9	71·3	*71·2*	*70·3*	73·1	72·1	73·2	71·1	73·4	71·2
Fa†	28·8	*28·9*	*28·7*	*71·7*	29·2	30·3	27·1	28·7	*28·8*	*29·7*	26·9	27·9	26·8	28·9	26·6	28·8
Fo range: low	70·8	*70·9*	*71·3*	*71·0*	70·9	69·0		71·0	*71·2*	*70·3*	72·9		72·4	70·8	73·4	70·7
high	72·0	*71·1*	*71·9*	*71·7*	70·7	70·5		71·3	*71·5*	*70·5*	73·5		73·7	71·6	73·8	71·4
No. of analyses	3	2	3	2	3	4	1	2	2	2	3	1	4	4	2	4

* All sample numbers have the prefix KEH.
† Italicized values of Fo and Fa were calculated after correcting for systematic errors in Fe concentration (too high by 3% relative) caused by a calibration error.
n.a., not analyzed. Analyses were made by wavelength-dispersive electron microprobe analysis at Stanford University and the University of California, Davis. Silicate minerals and metal oxides were used as calibration standards. Details of analytical procedures have been given by Brandriss (1993).

Table 3: Selected electron microprobe analyses of plagioclase

	Layered gabbros												
	Ordinary layered gabbros				Mafic macrolayers								
Sample:*	400	264B	424	424	280	280	280	402B	412	412	412	425	425
Analysis no:	2	6	6	7	55	53	52	54	4	2	3	3	5
Description:†	subhed	subhed	euhed core	rim of No. 6	subhed	emb core	rim of No. 53	subhed	chad in aug	euhed core	rim of No. 2	subhed core	interg
SiO_2	50·67	51·46	52·24	54·10	52·54	48·82	52·34	52·62	50·61	51·33	53·69	52·16	54·46
Al_2O_3	31·13	29·88	30·30	29·19	30·58	33·07	30·10	30·46	31·20	30·17	29·20	30·59	28·90
FeO	0·51	0·30	0·45	0·49	0·51	0·45	0·97	0·50	0·42	0·48	0·30	0·36	0·17
MgO	n.a.	n.a.	n.a.	n.a.	n.a.	n.a.	n.a.	n.a.	n.a.	n.a.	n.a.	n.a.	n.a.
CaO	14·01	12·80	13·06	11·47	12·72	15·82	12·54	13·02	14·28	13·41	11·88	12·9	11·22
Na_2O	3·57	4·05	3·99	4·99	4·28	2·42	4·04	3·91	3·35	3·78	4·55	4·08	4·97
K_2O	0·18	0·23	0·06	0·13	0·27	0·14	0·16	0·33	0·16	0·23	0·33	0·02	0·19
Total	100·07	98·72	100·10	100·37	100·90	100·72	100·15	100·84	100·02	99·40	99·95	100·11	99·91
An	67·7	62·7	64·2	55·5	61·2	77·7	62·6	63·6	69·5	65·3	57·9	63·5	54·9
Ab	31·2	35·9	35·5	43·7	37·3	21·5	36·4	34·5	29·5	33·3	40·2	36·4	44·0
Or	1·0	1·3	0·4	0·7	1·6	0·8	1·0	1·9	0·9	1·3	1·9	0·1	1·1

$^{87}Sr/^{86}Sr$ for the metabasaltic xenoliths range from 0·7034 to 0·7046 (for $t = 60$ Ma; Tegner *et al.*, 1998), consistent with derivation from the country rock lavas (Holm, 1988; Fram & Lesher, 1997). Initial ratios for plagioclase from a layered gabbro and a large ultramafic body are 0·7045 and 0·7047, respectively (for $t = 50$ Ma; Nevle *et al.*, 1994; Tegner *et al.*, 1998), and an initial ratio of approximately 0·7053 was calculated for a hornblende–andesine pegmatite dike. All values are within the ranges for early Tertiary basalts from the area (Holm, 1988; Fram & Lesher, 1997). The small variations in $(^{87}Sr/^{86}Sr)_i$ for the plutonic rocks may reflect variable amounts of contamination by the Tertiary metabasalts or Precambrian granitoid gneisses that host the intrusion (Pankhurst *et al.*, 1976; Holm, 1988; Kays *et al.*, 1989; Stewart & DePaolo, 1990; Fram & Lesher, 1997).

DISCUSSION

The discordant contacts of ultramafic and oxide gabbro bodies at Stand and Deliver Nunatak clearly indicate that the bodies formed or grew by postcumulus processes. The high temperatures of crystallization of the ultramafic rocks (roughly 1000–1100°C) indicate that they must have formed under magmatic conditions. The irregular or branching shapes of the ultramafic and oxide gabbro bodies, however, do not resemble dilational intrusive geometries. Instead, they are most easily interpreted as representing relict pathways along which metasomatizing liquids percolated through and reacted with the partially solidified cumulus pile. In the case of the small ultramafic and oxide gabbro bodies, the close spatial association with metabasaltic xenoliths suggests an obvious source for the reactive liquids: as Brandriss *et al.* (1996) demonstrated, the xenoliths were derived from hydrothermally altered country rocks, and must have expelled hydrous fluids or melts as they were heated. These hydrous fluids or melts would have been out of equilibrium with the cumulus mineral assemblage, as it has been demonstrated experimentally that addition of H_2O to mafic magmas destabilizes plagioclase relative to the ferromagnesian minerals (e.g. Yoder & Tilley, 1962; Helz, 1976; Beard & Lofgren, 1991; Sisson & Grove, 1993).

The postulated results of contamination are illustrated schematically in Fig. 17. We hypothesize that dehydration of the xenoliths produced pockets of hydrous fluid or melt that migrated through and reacted with the gabbroic cumulus pile. The high concentrations of H_2O caused resorption of plagioclase, resulting in formation of discordant bodies of ultramafic rock along the paths of flow. Where the hydrous liquids came to rest, they mixed with gabbroic cumulates and crystallized to form coarse-grained, massive bodies of oxide gabbro. In places where hydrous liquids were expelled from the xenoliths and

	Ultramafic bodies						Oxide gabbro bodies					Hornblende–andesine pegmatite dike	
	Large sheets					Small body	Large sheet				Small body		
Sample:*	303A	303C	303C	303C	406B	289	406C	413	413	414	288	303I	303I
Analysis no.:	3	5	4	1	1	2	4	7	8	55	52	6	5
Description:†	interg	chad in olivine	interg	interg	interg	interg	euhed	subhed core	subhed rim	subhed	euhed	subhed core	rim of No. 2
SiO_2	52·99	50·00	53·77	61·19	52·88	53·71	53·06	53·02	53·59	52·80	54·19	57·37	60·80
Al_2O_3	28·98	30·59	29·16	24·12	29·79	29·33	29·26	29·22	28·71	30·17	29·53	25·06	22·93
FeO	0·31	0·48	0·47	0·39	0·43	0·39	0·54	0·39	0·42	0·66	0·48	0·49	0·41
MgO	0·04	0·05	0·03	0·06	n.a.	0·11	n.a.	n.a.	n.a.	n.a.	n.a.	0·05	0·02
CaO	11·48	13·44	11·26	6·03	11·95	11·68	12·42	12·64	11·53	12·91	11·65	8·46	5·84
Na_2O	4·46	3·78	4·93	8·16	4·56	4·51	4·58	4·42	4·92	4·06	4·58	6·58	7·87
K_2O	0·42	0·13	0·37	0·50	0·28	0·35	0·34	0·21	0·34	0·34	0·39	0·47	0·70
Total	98·68	98·47	99·99	100·45	99·89	100·08	100·20	99·90	99·51	100·94	100·82	98·48	98·57
An	57·3	65·8	54·6	28·2	58·2	57·7	58·8	60·5	55·3	62·5	57·1	40·4	27·9
Ab	40·3	33·5	43·3	69·0	40·2	40·3	39·3	38·3	42·7	35·6	40·6	56·9	68·1
Or	2·5	0·8	2·1	2·8	1·6	2·1	1·9	1·2	1·9	2·0	2·3	2·7	4·0

* All sample numbers have the prefix KEH.
† euhed, euhedral; subhed, subhedral; emb, embayed; chad, chadacryst; interg, intergranular.
n.a., not analysed.

trapped immediately within the host cumulates, the contaminated cumulates recrystallized as rinds of oxide gabbro along xenolith surfaces. The striking petrological similarities between the small and large bodies suggest that the large bodies formed by similar metasomatic processes acting at a much larger scale. The mechanisms of formation for bodies of various sizes are considered in more detail below.

Evidence for a metasomatic origin

Field and textural relationships provide strong evidence for a metasomatic origin for the small ultramafic and oxide gabbro bodies. The extreme sharpness of the contacts between small ultramafic bodies and layered gabbros is a distinctive characteristic of metasomatic reaction fronts (Korzhinskii, 1965, 1970; Hofmann, 1972). These contacts are interpreted to represent advancing surfaces of equal chemical potential, inside which plagioclase was destabilized during reaction between gabbroic cumulates and a plagioclase-undersaturated liquid. In bodies with olivine-rich cores (in which pyroxene is interstitial), the boundary between pyroxene-rich and olivine-rich zones is interpreted to represent a second reaction front marking the disappearance of pyroxene.

In accord with this interpretation, the geometries of the zoned ultramafic bodies (consisting of elongate, olivine-rich cores surrounded by pyroxene-rich halos; Fig. 8a) are suggestive of formation by coupled processes of infiltrative and diffusive metasomatism. The general pattern of zoning is similar to that produced around metasomatic veins in hydrothermal systems, where large-scale advective transport of components through fractures produces mineral assemblages that do not vary for long distances along the fractures, whereas smaller-scale diffusive transport into the surrounding rock produces reaction fronts that are closely spaced along perpendicular traverses (Norton & Knapp, 1977). In the ultramafic bodies, the olivine-rich cores are interpreted to represent the former traces of permeable channelways within the cumulus pile, with pyroxene-out and plagioclase-out surfaces representing diffusive metasomatic fronts that migrated outward into the adjacent gabbro. The preferential

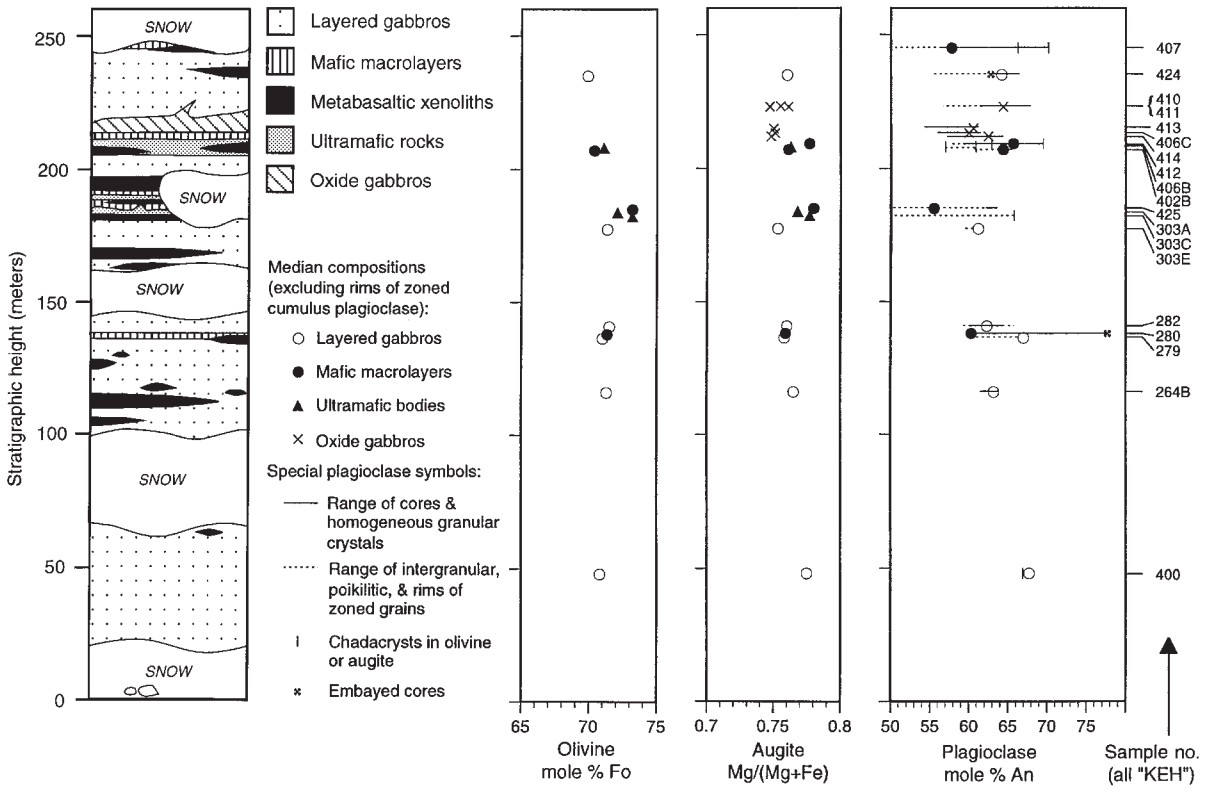

Fig. 14. Stratigraphic section with mineral compositions, Stand and Deliver Nunatak. The approximate trend of the section is shown in Fig. 2. The range of olivine and augite compositions in each sample is less than the width of the symbol.

deflection of bodies along planes of layering and lamination indicates that these planes were the directions of highest permeability.

The close spatial association of ultramafic and oxide gabbro bodies provides further evidence for a metasomatic origin. The oxide gabbros, being relatively rich in feldspar and poor in ferromagnesian silicates, are enriched in components that were excluded from the ultramafic bodies. Such a complementary association of rock types is consistent with processes of infiltration metasomatism (Korzhinskii, 1970). In the case of the large sheet-like bodies (for which bulk compositions have been obtained), mass balance constraints (Fig. 18) suggest that the ultramafic and oxide gabbro bodies could have formed by metasomatic segregation of a mafic macrolayer precursor, producing ultramafic rock and oxide gabbro in a ratio of roughly two to one.

Textural features of the ultramafic bodies are consistent with a metasomatic origin. In the pyroxene-rich ultramafic bodies, the pyroxene grains typically have interdigitating or consertal boundaries, and there is commonly extensive replacement of olivine by orthopyroxene. These features are suggestive of grain boundary migration and mineral–melt reaction, both consistent with processes of textural and chemical re-equilibration associated with metasomatism. Preservation of these textures in pyroxene-rich zones suggests that re-equilibration did not proceed to completion. In contrast, the poikilitic textures of olivine-rich zones are characteristic of a close approach to equilibrium (Hunter, 1987), consistent with the hypothesis that the olivine-rich zones represent anomalously permeable channels through which there were higher fluxes of metasomatizing liquid.

Nature and source of the metasomatizing liquid

Given their anomalous mineral parageneses, it is clear that the ultramafic and oxide gabbro bodies crystallized from liquids that were chemically distinct from 'normal' pore liquids in the layered gabbros. In the ultramafic bodies, the absence of plagioclase and the unusually high abundances of hydrous phases (hornblende and phlogopite) suggest that the liquid was anomalously rich in H_2O. In addition to being an essential component of hydrous minerals, H_2O destabilizes plagioclase relative to mafic minerals in basaltic magmas (Yoder & Tilley,

Table 4: Whole-rock compositions

	Layered gabbros						Ultramafic bodies			Oxide gabbro body			Hornblende–andesine pegmatite dike*		
	Ordinary layered gabbros			Mafic macrolayers			Large sheets		Small body	Large sheet					
Sample:†	264B	400	424	402B	412	425	303A	406B	289	406C	413	414	303I-1	303I-2	Av.
SiO_2	47·43	49·44	48·12	40·75	37·08	38·34	37·19	36·93	43·88	42·85	42·66	47·74	61·47	64·18	62·83
TiO_2	0·75	0·62	0·87	1·91	1·76	1·25	1·76	1·78	2·53	3·25	3·23	1·61	1·34	1·07	1·21
Al_2O_3	14·31	18·80	16·12	6·89	5·60	4·07	2·71	2·98	4·38	14·58	13·85	16·57	15·97	15·84	15·91
Fe_2O_3‡	10·56	6·47	9·03	22·08	25·05	24·32	26·35	26·76	17·80	17·07	17·78	11·05	4·93	4·19	4·56
MnO	0·17	0·11	0·15	0·30	0·32	0·34	0·33	0·37	0·27	0·17	0·18	0·15	0·07	0·06	0·07
MgO	12·04	7·78	9·31	18·79	22·33	26·28	26·29	25·15	17·15	6·53	6·62	7·68	2·25	1·47	1·86
CaO	12·93	15·09	13·06	7·62	5·34	3·73	3·53	4·36	12·80	12·97	12·56	12·96	4·00	2·81	3·41
Na_2O	1·71	2·17	2·15	0·65	0·68	0·60	0·29	0·40	0·48	2·10	2·13	2·61	6·55	7·65	7·10
K_2O	0·11	0·14	0·25	0·14	0·05	0·15	0·22	0·11	0·08	0·22	0·32	0·36	2·68	1·98	2·33
P_2O_5	0·02	0·02	0·05	0·05	0·02	0·07	0·12	0·04	0·07	0·02	0·04	0·04	0·37	0·26	0·32
Total	100·03	100·64	99·11	99·18	98·23	99·15	98·79	98·88	99·44	99·76	99·37	100·77	99·63	99·51	99·57
Zn	66	41	61	133	154	166	191	193	112	109	100	55	35	26	30
Cu	275	150	138	233	247	119	202	135	1102	312	897	36	34	19	26
Ni	240	114	199	716	678	804	873	742	541	230	168	88	44	19	31
Cr	319	159	392	1071	1495	1846	2291	1842	895	6	56	120	42	5	23
V	183	176	181	447	538	316	450	518	459	875	934	390	127	71	99
Ba	40	45	93	63	26	41	11	29	47	67	119	87	683	457	570
Nb	1	1	3	6	2	5	6	4	10	3	9	5	73	78	76
Zr	17	18	33	46	13	34	40	36	57	32	72	56	774	949	861
Y	9	7	10	10	5	6	8	8	19	10	14	10	49	47	48
Sr	306	394	360	144	127	109	55	54	74	355	330	441	198	117	158
U	b.d.	b.d.	b.d.	1	b.d.	b.d.	1	b.d.	b.d.	b.d.	b.d.	b.d.	3	4	3
Rb	b.d.	b.d.	4	2	b.d.	2	6	2	1	4	6	8	50	36	43
Th	1	1	b.d.	1	b.d.	b.d.	b.d.	b.d.	b.d.	2	b.d.	b.d.	12	17	14
Pb	4	2	3	5	3	3	6	3	4	3	7	3	6	6	6
Ga	15	17	17	12	10	8	8	8	10	22	22	19	20	21	20
Hf	1						1						16	20	18
Ta	1						1						7	7	7
Co	70						176						40	31	35
Sc	37						20						10	6	8
La	2·3						5·1						78·3	80·6	79·5
Ce	6·3						10·9						151	155	153
Sm	1·37						1·67						11·4	10·1	10·8
Eu	0·61						0·37						2·30	1·79	2·05
Tb	0·24						0·23						1·43	1·26	1·35
Yb	0·65						0·85						4·22	4·47	4·35
Lu	0·11						0·13						0·56	0·59	0·58

* Analyses of two separate 0·5 kg pieces of a single dike, and average of the two analyses.
† All sample numbers have the prefix KEH.
‡ All Fe as Fe_2O_3.
Oxides are in wt %, elements are in ppm. b.d., below detection. Th, Hf, Ta, Co, Sc, and REE by INAA at Kansas State University, using methods adapted from Gordon *et al.* (1968) and Jacobs *et al.* (1977); the accuracy of these methods has been reported by Cullers *et al.* (1979). All other elements by XRF at Stanford University, using a fused disk method based on the technique of Norrish & Hutton (1969) for major elements and a pressed powder method based on the technique of Norrish & Chappell (1977) for trace elements.

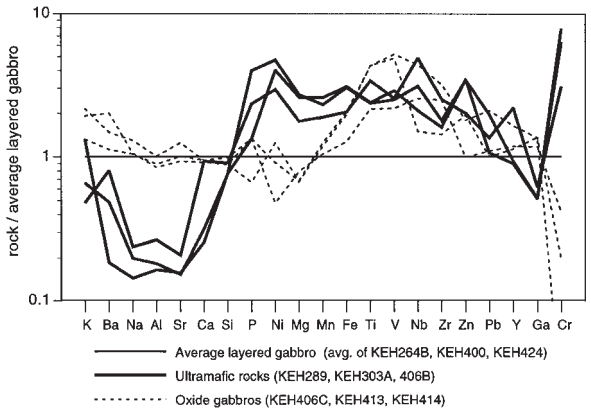

Fig. 15. Spider diagrams of whole-rock ultramafic and oxide gabbro samples, normalized to average ordinary layered gabbro. Elements are grouped according to their tendency to partition into different minerals.

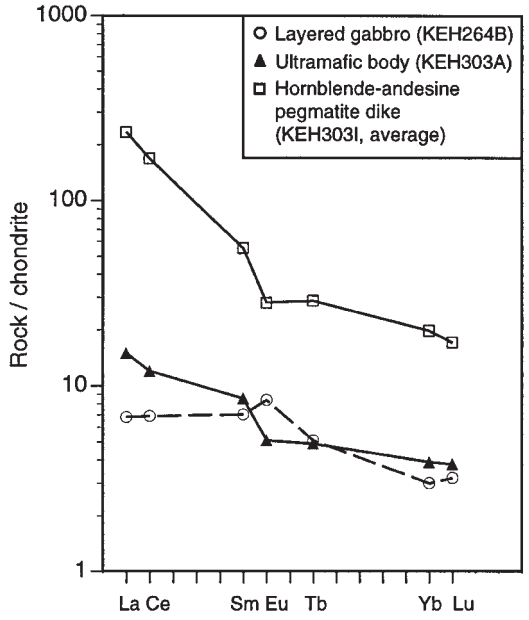

Fig. 16. Chondrite-normalized REE analyses.

1962; Holloway & Burnham, 1972; Helz, 1976; Spulber & Rutherford, 1983; Beard & Lofgren, 1991; Sisson & Grove, 1993; Gaetani *et al.*, 1994). Addition of H_2O to a gabbroic cumulate would thus cause resorption of plagioclase, producing bodies of ultramafic rock. Dilution of the hydrous liquid by dispersion and mixing with 'normal' intercumulus melts would eventually produce a magma of intermediate H_2O content in which plagioclase would again be stable, resulting in the formation of discordant plagioclase-bearing rocks such as the oxide gabbros. A hydrous metasomatizing liquid provides an attractive explanation for the coarse-grained to pegmatitic textures of the oxide gabbros, as the development of such textures in mafic rocks is commonly associated with locally elevated concentrations of magmatic H_2O (e.g. Puffer & Horter, 1993; Larsen & Brooks, 1994; Mitchell *et al.*, 1997). The ultramafic and oxide gabbro bodies are thus interpreted as two distinct products of interaction between gabbroic cumulates and hydrous pore liquids.

As outlined previously, the close spatial association between postcumulus bodies and metabasaltic xenoliths suggests that the xenoliths were the source of H_2O in the metasomatizing liquids. In the case of the small bodies, the tight clustering around xenolith contacts indicates that contamination with H_2O must have occurred *in situ*. In the case of the large sheet-like bodies, it is possible that some contamination may have occurred elsewhere in the pluton or during transit of magmas through the hydrothermally altered crust, with hydrous contaminated magmas having then deposited their suspended phenocrysts at the floor of the magma chamber. The large sheet-like ultramafic bodies might thus have originated as cumulus layers, containing anomalously hydrous pore liquids that eventually escaped into and reacted with ordinary gabbroic cumulates deposited on top of them. This would account for the broadly stratiform but locally transgressive contacts between ultramafic sheets and layered gabbros. Abundant evidence for episodic replenishment of the Kap Edvard Holm magma chamber (e.g. Bernstein *et al.*, 1992; Tegner *et al.*, 1993; Bird *et al.*, 1995) is consistent with this hypothesis, as it provides a mechanism for the deposition of 'dry' uncontaminated cumulates atop a hydrous, contaminated cumulus mush.

An influx of hydrous plagioclase-undersaturated magma provides an explanation for the gradual upward progression from ultramafic layers to mafic macrolayers and, ultimately, to plagioclase-rich gabbroic layers. Initially, a pile of ultramafic cumulates may have formed from phenocrysts that were carried by a plagioclase-undersaturated magma and deposited on the magma chamber floor. As the hydrous magma mixed with resident magma, or with subsequent influxes of magma, the H_2O concentration decreased by dilution and plagioclase returned to the liquidus. Such a transition from plagioclase-undersaturated to plagioclase-saturated conditions may be recorded by the presence in mafic macrolayers of plagioclase grains with small embayed cores. These cores could be the remnants of crystals that were partially resorbed when the magma was contaminated with H_2O, and were then mantled by new growth as magma mixing proceeded and H_2O concentrations decreased by dilution.

An alternative that must be considered is the possibility that the ultramafic sheets formed from pulses of relatively primitive (picritic?) magma. Such magmas might flow into a dominantly gabbroic magma chamber and deposit olivine-rich cumulates on the chamber floor (e.g. Huppert

Table 5: Strontium isotope analyses of rocks and minerals from Stand and Deliver Nunatak

Sample	Description	$^{87}Sr/^{86}Sr$	Rb (ppm)	Sr (ppm)	$(^{87}Sr/^{86}Sr)_i$*
KEH264B	Layered gabbro: plagioclase separate†	0·704513±9	<1	>306	
KEH303A	Large sheet-like ultramafic body; plagioclase separate†	0·704680±8	<6	>55	
KEH303B	Metabasalt xenolith underlying KEH303A; plagioclase separate†	0·704622±7	<1	>135	
KEH259A	Metabasalt xenolith; plagioclase separate†	0·703825±8	<1	>134	
KEH274D	Metabasalt xenolith; plagioclase separate†	0·703404±7	<1	>216	
KEH303I	Hornblende–andesine pegmatite dike; whole-rock	0·705945±10	36	117	0·7053
KEH303I	Hornblende–andesine pegmatite dike; saussuritized plagioclase separate†	0·705817±9	?	?	

* Model initial value, calculated for an age of 50 Ma (Nevle *et al.*, 1994; Tegner *et al.*, 1998).
† Plagioclase is assumed to have lower Rb and higher Sr than analyzed whole rocks, thus establishing the limits shown in the table. [Whole-rock compositions of xenoliths have been given by Brandriss *et al.* (1996).] Assuming ages of 50 Ma for the plutonic rocks (Nevle *et al.*, 1994; Tegner *et al.*, 1998) and 60 Ma for the metabasalts (Tegner *et al.*, 1998), the initial isotopic ratios are probably within 0·00005 of the measured ratios for all samples other than KEH303I.

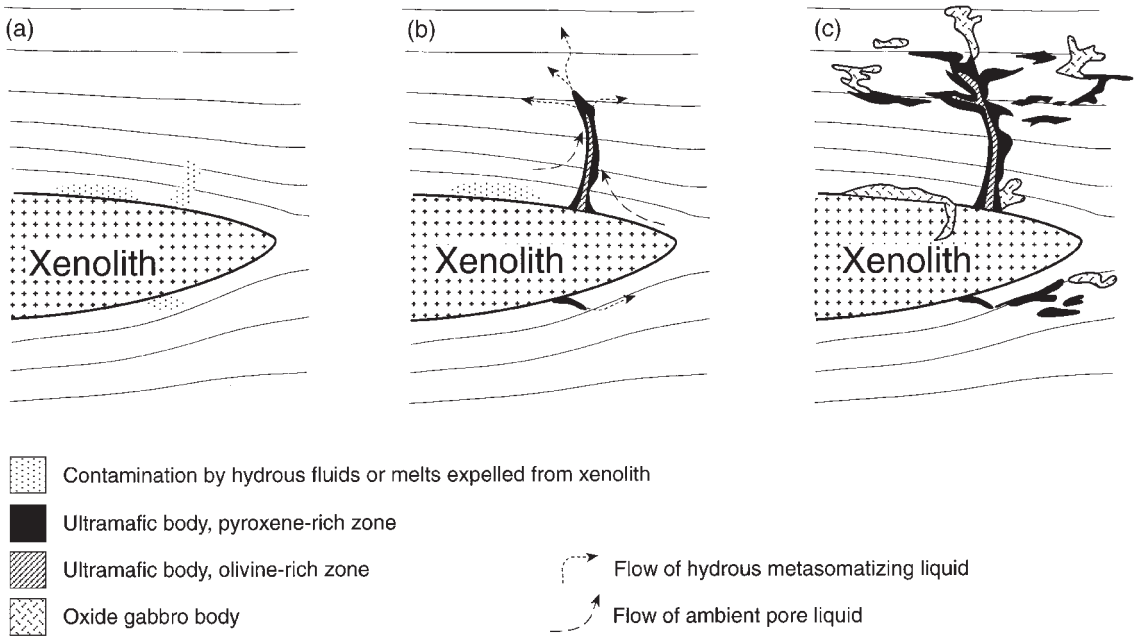

Fig. 17. Schematic illustration of the process postulated to have formed the small ultramafic and oxide gabbro bodies. (a) A metabasaltic xenolith is trapped in the cumulus pile and contaminates the host gabbro with H_2O during devolatilization or partial melting. (b) The hydrous liquid resorbs plagioclase as it infiltrates the partially molten cumulates, leaving ultramafic solid residua. As resorption of cumulates proceeds, the increase in volume as a result of melting produces localized overpressures (Sonnenthal & McBirney, 1998), causing hydrous liquid to be driven outward in all directions. Much of the flow is directed upward because of the low densities of the hydrous melts. Ultramafic bodies grow along the paths of flow, and in the cores of some bodies, H_2O concentrations are high enough to cause complete resorption of pyroxene, resulting in the formation of olivine-rich zones. Ambient pore liquids are drawn into the zones of metasomatism as hydrous melts are advected away. (c) The migrating hydrous liquids are progressively diluted as they mix and react with gabbroic cumulates and ambient pore liquids; the mixtures eventually crystallize as bodies of oxide gabbro.

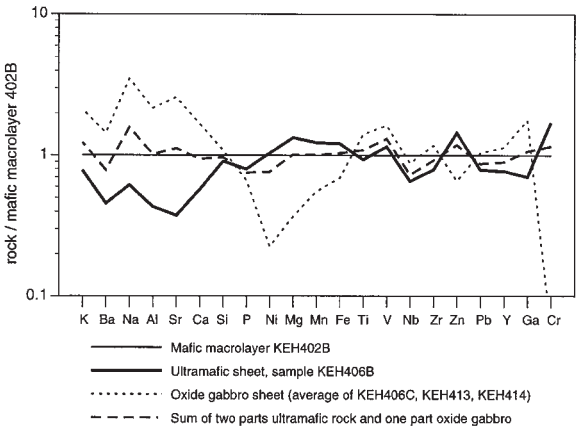

Fig. 18. Spider diagram of whole-rock samples of large sheet-like ultramafic and oxide gabbro bodies, normalized to the composition of a mafic macrolayer (sample KEH402B) exposed along strike at approximately the same stratigraphic level. Shown also is a composition representing a mixture of two parts ultramafic rock to one part oxide gabbro. Relative to concentrations in the mafic macrolayer, elements that are enriched in the oxide gabbros are depleted in the ultramafic rock and vice versa. It should be noted also that the 2:1 mixture crudely approximates the mafic macrolayer composition. These features suggest that the ultramafic and oxide gabbro sheets could have formed by segregation from an initially homogeneous mafic macrolayer, producing the two rock types in a ratio of roughly two to one.

& Sparks, 1980; Emeleus, 1987; Robins *et al.*, 1987). Alternatively, such magmas might intrude or infiltrate gabbroic cumulus piles as semi-conformable sills (Bédard *et al.*, 1988; Juteau *et al.*, 1988; Laurent *et al.*, 1991; Bernstein *et al.*, 1992; Tegner & Wilson, 1993; Bédard & Hébert, 1996; Tegner & Robins, 1996). The best evidence for such processes would be the preservation of primitive compositional features in the constituent minerals. For example, Bernstein *et al.* (1992) described melanocratic layers in other parts of the Kap Edvard Holm Complex in which augites were anomalously rich in Cr, and attributed this to crystallization from sills of relatively primitive magma. Similarly, in ophiolitic gabbros that are intruded by late dikes and sills of primitive wehrlite, mafic silicates in the wehrlites typically are strongly magnesian regardless of the compositions of minerals in the host gabbros (e.g. Juteau *et al.*, 1988; Laurent *et al.*, 1991; Bédard & Hébert, 1996). In view of such observations, emplacement of primitive magma seems an unlikely explanation for the Stand and Deliver ultramafic sheets, given: (1) the absence of mafic minerals of anomalously primitive composition; (2) the nearly identical compositions of mafic minerals in the ultramafic bodies and host layered gabbros; (3) the remarkable petrological similarities between the large sheet-like bodies and the smaller bodies, the latter of which clearly formed *in situ* without involvement of an externally derived magma. Thus, as there is no strong evidence for involvement of a primitive magma, formation from hydrous gabbroic magmas seems the most likely origin for ultramafic sheets at Stand and Deliver Nunatak.

Given this conclusion, the sheet-like oxide gabbro body (Figs 2 and 10) is most logically interpreted to represent a zone of mixing between partially molten gabbroic cumulates and the hydrous metasomatizing liquids that escaped from the underlying ultramafic sheet, via a process analogous to that outlined in Fig. 17. As hydrous liquids segregated from the ultramafic layer and dispersed into larger volumes of cumulates (forming masses of oxide gabbro), they became progressively diluted until their compositions approached those of 'normal' intercumulus liquids. At this point the metasomatizing capability of the liquids was lost and growth of the oxide gabbro body ceased. Localized segregation and migration of the metasomatizing liquids probably accounts for the heterogeneity of the large oxide gabbro body, with the variety of whole-rock compositions probably reflecting outcrop-scale variations in the proportions of pore liquids and cumulus minerals. The extremely low concentration of Cr in sample KEH406C (Table 4), for example, suggests that this rock formed largely from a pocket of liquid, which would have been depleted in chromium as a result of magnetite fractionation before segregation. Speculatively, the composition of this rock may approximate that of a liquid, in which case the high Fe content (17 wt % total Fe as Fe_2O_3) would imply earlier crystallization along an Fe enrichment trend.

Quantitative constraints

To examine more rigorously the effects of H_2O on phase relationships in gabbroic cumulates, we have made thermodynamic calculations using the MELTS software package of Ghiorso & Sack (1995). These calculations place constraints on the proposed metasomatic process, including an estimate of the amount of water required to resorb all of the plagioclase in a mass of partially molten gabbroic cumulates.

First, model pore liquid compositions were determined by calculating the compositions of liquids in equilibrium with the cumulus minerals in 'normal' gabbroic cumulates. This was done by: (1) starting with whole-rock analyses of ordinary layered gabbros (presumed to represent mixtures of cumulus minerals plus crystallized pore liquids); (2) adding small amounts of H_2O (an essential component largely excluded from the final solid assemblage, but which must have been present in the pore liquids); (3) calculating the equilibrium liquid compositions at small degrees of 'melting', such that the liquid compositions are constrained to be in equilibrium with minerals having roughly the compositions of the major cumulus phases (i.e. the abundances and compositions of minerals in the calculated solid assemblages should be

very similar to those of the actual minerals in the rocks). We assumed a temperature of 1100°C (slightly higher than the final temperatures of equilibration recorded by pyroxenes in the ultramafic bodies), a pressure of 2 kbar, and oxygen fugacities buffered at quartz–fayalite–magnetite equilibrium (QFM) or one order of magnitude higher (QFM + 1). The water contents of the initial systems were varied by trial and error to achieve concentrations of roughly 1–1·5 wt % in the calculated liquids (a reasonable range for moderately evolved mafic liquids). Calculations were performed using samples KEH264B, KEH400, and KEH424 as model cumulates. Results are summarized in Table 6.

For all three samples, the observed primary mineral assemblage in the layered olivine gabbros could be reproduced fairly well at an oxygen fugacity near QFM equilibrium (Table 6). At higher oxygen fugacities, however, the results were much poorer: the calculated assemblages at QFM + 1 contained orthopyroxene and abundant magnetite (unlike the ordinary layered gabbros), as well as an olivine more magnesian than the one observed (one example is shown in Table 6). Oxygen fugacities near QFM were therefore used for all calculations. For all three samples, the calculated initial pore liquids at QFM had compositions roughly equivalent to basaltic andesite or mugearite, with 52–53% silica and ~3% MgO (Table 6). It is important to emphasize that these compositions must be regarded as rough approximations, given the lack of precise constraints on temperature, oxygen fugacity, and magmatic water content. Because the compositions are thermodynamically and petrologically reasonable, however, they are considered suitable for use in quantifying the effects of adding H_2O to the system.

The effects of adding H_2O to partially molten cumulates were simulated by 'adding' H_2O incrementally to mixtures of 50% cumulus minerals (approximated by whole-rock compositions) and 50% pore liquid (calculated at QFM). Equilibrium assemblages were recalculated after each incremental addition of H_2O. Results for the three model compositions are summarized in Fig. 19. The calculations predict that as H_2O is added, plagioclase will be resorbed readily, with all plagioclase disappearing after the addition of 1–1·5 wt % H_2O. The mafic minerals are resorbed more gradually, with the ratio of olivine to augite decreasing throughout the interval of plagioclase resorption. In systems that contain little olivine initially, olivine may disappear temporarily from the solid assemblage (e.g. KEH400). Upon the disappearance of plagioclase, the solid residuum has the composition of pyroxenite ± olivine, a rough analogue for the pyroxene-rich zones of ultramafic bodies. After all plagioclase has been resorbed, the continued addition of water stabilizes olivine relative to pyroxene, so that as fluid saturation is approached, augite disappears entirely and olivine becomes the only stable solid phase. The most strongly hydrated systems should thus resemble the olivine-rich zones of ultramafic bodies, consistent with the hypothesis that these zones represent anomalously permeable conduits in which H_2O concentrations were highest and liquid fluxes were greatest. It is also consistent with experiments in hydrous basaltic systems, in which olivine ± magnetite are commonly the last solid phases to disappear as H_2O concentrations are increased (Holloway & Burnham, 1972; Spulber & Rutherford, 1983; Sisson & Grove, 1993; Gaetani *et al.*, 1994). The persistence of magnetite to high water concentrations is not predicted by the calculations, suggesting that the abundant magnetite found in ultramafic rocks at Stand and Deliver Nunatak may have been stabilized by oxygen fugacities that were slightly higher than those used in the calculations.

The model calculations predict that as H_2O is added to each system, resorption of ferromagnesian silicates should cause residual mafic grains to be enriched in Mg relative to Fe (Fig. 19). Because no such enrichment is observed in the ultramafic bodies, we must assume (if our metasomatic model is correct) that the Mg/Fe ratios of the mafic silicates were controlled by equilibration with large amounts of pore liquid, rather than by the Mg and Fe contents of the original solid residua. This implies that the amounts of pore liquid that passed through the ultramafic bodies were substantially greater than the masses of the solid mafic residua, suggesting a highly focused flow of liquids through anomalously permeable channels. We hypothesize that pore liquids from the surrounding cumulates were drawn into the ultramafic bodies as the metasomatizing liquids advected away, so that over time, the liquids in the ultramafic bodies became more similar in composition to the uncontaminated pore liquids in surrounding cumulates. This provides an explanation for the nearly identical compositions of mafic minerals in gabbroic and ultramafic rocks, and for the similarity between the compositions of intergranular plagioclase grains in ultramafic bodies and the rims of zoned plagioclase grains in layered gabbros.

Significance of mafic mineral assemblages

In the pyroxene-rich ultramafic rocks, the appearance of abundant magnetite coincides roughly with the growth of orthopyroxene at the expense of olivine and augite. These relationships are strikingly similar to those produced during intercumulus crystallization in the layered gabbros, where magnetite and orthopyroxene appear as intergranular crystals and late orthopyroxene locally replaces augite and olivine. This crystallization sequence is also commonly encountered during fractionation of tholeiitic basalts, in which the cessation of olivine crystallization typically coincides approximately with the first

Table 6: Calculated compositions of pore liquids and minerals in three ordinary layered gabbros at 1100°C, 2 kbar

Sample:	KEH264B	KEH400	KEH424	
Oxygen fugacity:	QFM	QFM	QFM	QFM+1
*Liquid compositions**				
SiO_2	53·04	52·04	53·46	55·93
TiO_2	1·60	1·32	1·69	1·18
Al_2O_3	16·93	17·29	16·84	18·16
Fe_2O_3	1·78	1·85	1·75	1·72
FeO	9·33	9·64	9·07	5·26
MgO	3·43	3·47	3·28	3·24
CaO	6·16	6·22	5·98	5·28
Na_2O	4·92	5·28	4·89	5·33
K_2O	1·48	1·40	1·87	2·62
H_2O†	1·33	1·48	1·16	1·29
Mineral compositions				
Olivine (% Fo)	70	71	69	79
Augite [Mg/(Mg+Fe)]	0·72	0·73	0·72	0·75
Pigeonite [Mg/(Mg+Fe)]	0·69			
Orthopyroxene [Mg/(Mg+Fe)]				0·79
Plagioclase (% An)	64	66	62	60
Phase proportions (wt %)				
Liquid	2·3	3·4	5·3	3·9
Olivine	15·4	5·3	9·6	2·4
Augite	42·4	40·5	40·0	40·2
Pigeonite	1·1			
Orthopyroxene				6·5
Plagioclase	37·5	50·5	43·5	42·7
Magnetite	1·3	0·4	1·6	4·4

* Minor components that are not listed (e.g. MnO, NiO) were excluded from the calculations because the MELTS program does not model their solution properties in the crystallizing solid phases.
† Water contents were chosen by trial and error to achieve concentrations of 1·0–1·5 wt % in the calculated liquid (see text).
Calculations were made using the MELTS software package of Ghiorso & Sack (1995). (See text for details).

appearances of magnetite and low-Ca pyroxene (e.g. Wager & Deer, 1939; Carmichael, 1964; Ghiorso, 1997). The appearance of intergranular orthopyroxene and magnetite in the layered gabbros might thus have resulted from late-stage fractionation of pore liquids, with the high abundances of these minerals in ultramafic bodies having resulted from crystallization of pore liquids that were drawn into zones of metasomatism. High concentrations of H_2O in these zones may also have stabilized magnetite relative to the silicates, perhaps accounting for the high abundances of magnetite in ultramafic and oxide gabbro bodies.

It is also possible that the formation of abundant orthopyroxene and magnetite in ultramafic rocks was facilitated by oxidation of the system during metasomatism. This would foster reactions of the type

$$3Fe_2SiO_4 + \tfrac{1}{2}O_2 = Fe_3O_4 + 3FeSiO_3.$$

Relatively oxidizing conditions may have developed as a result of assimilation of oxidized material from the metabasaltic xenoliths (e.g. Osborn, 1959; Juster *et al.*, 1989), a possibility supported by the observation that altered country rock basalts in the region commonly contain abundant ferric iron bound in secondary epidote

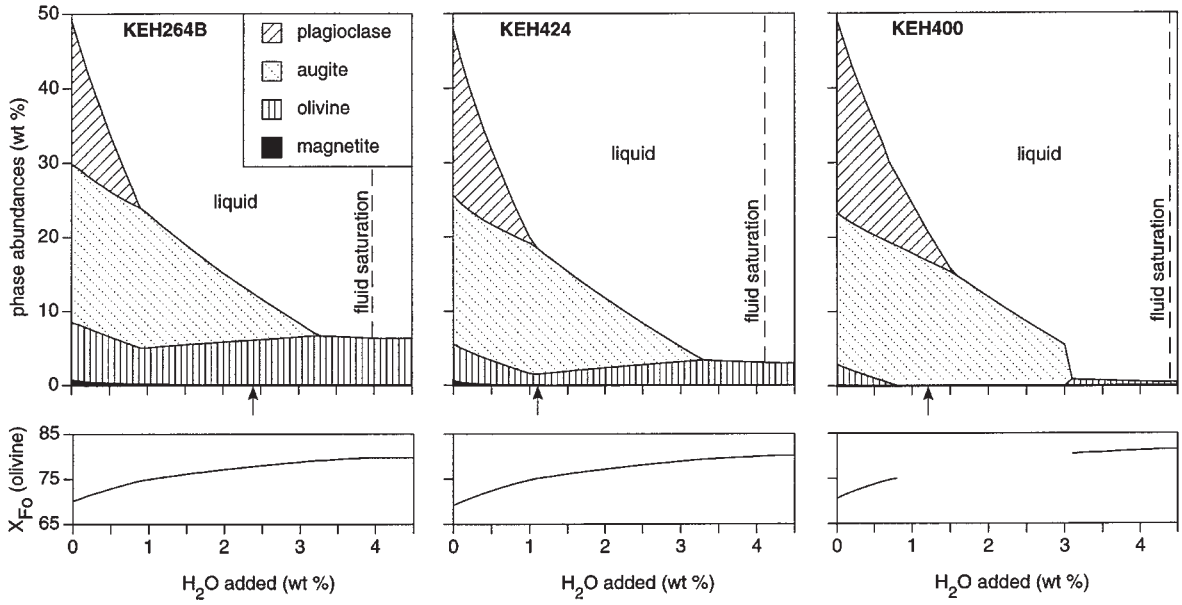

Fig. 19. Results of calculations simulating the effects of adding H_2O to 50:50 mixtures of pore liquid and cumulus minerals for three samples of ordinary layered gabbro from Stand and Deliver Nunatak (the calculated initial liquids have H_2O contents of 1·16–1·48 wt %; see text and Table 6). The upper graphs indicate equilibrium proportions of phases, and the lower graphs show predicted olivine compositions. Small arrows indicate the water contents above which magnetite is fully resorbed; fluid saturation lines indicate saturation with pure H_2O.

and prehnite (Bird *et al.*, 1985). Other possible mechanisms of oxidation include: (1) closed-system crystallization within the cumulus pile, with postcumulus growth of minerals rich in ferrous iron (olivine + augite) producing residual liquids enriched in oxygen (e.g. Ghiorso & Carmichael, 1985); (2) dissociation of H_2O, coupled with diffusive loss of H_2 (Sato, 1978); (3) evolution and loss of a fluid phase capable of scavenging reduced species of carbon (e.g. Mathez, 1984, 1989). Degassing of sulfate, conversely, could have produced late-stage fluids that were relatively reduced (Carmichael & Ghiorso, 1986), in which case the olivine-rich cores of ultramafic bodies might represent zones that were saturated in the reduced fluid whereas the orthopyroxene-rich halos represent zones that were oxidized by the escaping sulfate. Interestingly, ultramafic sample KEH289 has an anomalously high concentration of Cu (presumably in sulfide), suggesting that redox equilibria involving sulfur may have been important. Although such speculations are interesting, however, it is unclear whether oxidation reactions were necessarily a part of the metasomatic process.

The significance of the augite + magnetite assemblage in the oxide gabbros is unclear, but it may reflect complex relationships between bulk composition and oxygen fugacity. Assuming that the oxide gabbros formed from mixtures of metasomatizing liquids and gabbroic cumulates, the proportion of liquid to cumulus minerals would probably have been greater in oxide gabbros than in ordinary layered gabbros, causing the bulk compositions of oxide gabbros to be slightly more evolved. In the oxide gabbros, this is reflected in the slightly lower anorthite contents of plagioclase (Table 3, Fig. 14), the higher whole-rock concentrations of incompatible elements (e.g. Zr, Y, Ba, K; Table 4, Fig. 14), and the lower Cr contents of augites and bulk rocks (Table 4). Relatively evolved bulk compositions of oxide gabbros may also account for the disappearance of olivine and the crystallization of augite + magnetite: in experiments, Toplis & Carroll (1995) found that a tholeiitic liquid initially saturated in olivine + augite + plagioclase at ~1100°C would shift abruptly toward saturation in magnetite + augite + plagioclase if separated from its olivine-bearing solid residuum. By analogy, development of the augite + magnetite assemblage in the oxide gabbros may have occurred by increasing the ratio of pore liquid to cumulus minerals to an extent sufficient to have caused resorption of olivine. Toplis & Carroll (1995) noted that the transition from an olivine-bearing assemblage to an augite + magnetite assemblage was favored by increased oxygen fugacity, but would proceed eventually during cooling under conditions buffered at QFM. Thus, although formation of the oxide gabbro bodies may have been facilitated by high oxygen fugacities, it is uncertain whether this was a necessary condition.

A plausible argument in favor of relatively oxidized magmas can be made from the observation that augite in the oxide gabbros is almost identical in composition to augite in the layered gabbros. This suggests that the MgO/FeO ratio of the oxide gabbro magma was not greatly different from that of the normal pore liquid, and that magnetite precipitation therefore did not result from extended fractionation. This is very different from the situation observed in another well-studied system, ODP Site 735 on the Southwest Indian Ridge, where oxide gabbros infiltrated and locally replaced oxide-poor gabbroic cumulates (Dick *et al.*, 1991). At Site 735, oxide gabbros formed mainly from highly evolved liquids (Dick *et al.*, 1991), suggesting that magnetite saturation was delayed because of crystallization under relatively reducing conditions (probably near QFM; Natland *et al.*, 1991). The much earlier appearance of abundant magnetite in the oxide gabbros at Stand and Deliver Nunatak could thus be construed to reflect crystallization under relatively oxidizing conditions.

Formation of the pegmatitic dikes

The course of late-stage crystallization may be elucidated by examining more closely the hornblende–andesine pegmatite dikes, which represent segregations of the latest liquids in the fractionation sequence. When the composition of a pegmatite dike is plotted on an AFM diagram, it falls far to the iron-depleted side of typical tholeiitic fractionation trends (Fig. 20). Assuming the dikes represent pockets of trapped liquid, it is plausible that a whole-rock composition might approximate a liquid composition, in which case the high silica content (~63%), low Fe content (4–5% as Fe_2O_3), and moderate ratio of Fe/Mg would suggest that the final stages of fractionation involved rapid depletion of iron. This depletion may have resulted from the formation of abundant magnetite in the host oxide gabbros or ultramafic bodies. Crystallization of abundant magnetite might reflect crystallization under conditions that were substantially more hydrous (Sisson & Grove, 1993) and/or more oxidizing (Osborn, 1959; Ghiorso, 1997) than those typical of tholeiitic magmas.

Calculations made using the MELTS software package indicate that a residual liquid very similar in composition to pegmatite sample KEH303I can be formed from a mixture of gabbroic cumulus minerals and an Fe-rich (~13 wt % Fe as FeO) pore liquid, by allowing the system to cool to ~1020°C under oxidizing conditions (QFM + 2). Conversely, calculations suggest that at oxygen fugacities corresponding to the QFM buffer, crystallization cannot produce liquid residua as rich in silica and poor in iron as the pegmatitic dikes. It is important to emphasize that the results of these calculations cannot be construed as proof of crystallization under particular conditions, given the lack of precise constraints on the natural system. The calculations do, however, suggest that the more oxidized crystallization path is plausible and perhaps more likely. The pegmatites may thus be interpreted as late-stage residual liquids that were produced by crystallization of a mixture of cumulus minerals and a distinctly oxidized metasomatizing liquid. This possibility, combined with the evidence for hydration of the gabbroic cumulates, suggests that contamination of the Kap Edvard Holm magma by hydrous, oxidized metabasaltic country rocks may have shifted the liquid line of descent from a tholeiitic trend of iron enrichment toward a calc-alkaline trend of silica enrichment and iron depletion. This speculative interpretation is consistent with the observation that magnetite is a widespread minor cumulus phase throughout much of the Kap Edvard Holm Complex (Deer & Abbott, 1965; Wager & Brown, 1967; Elsdon, 1971*a*; Abbott & Deer, 1972).

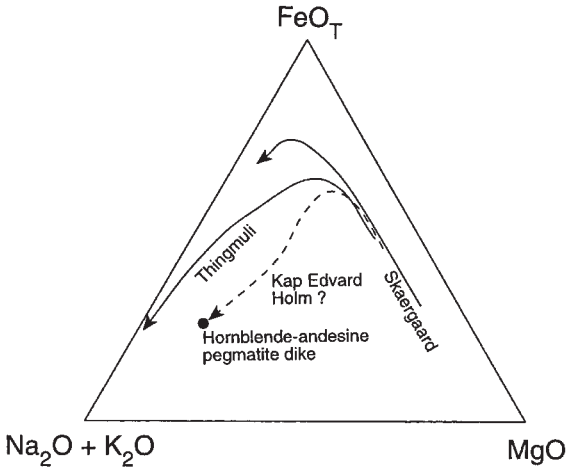

Fig. 20. Composition of a hornblende–andesine pegmatite dike (sample KEH303I) plotted on an AFM diagram, with lines representing the liquid lines of descent for the Skaergaard intrusion (Wager & Brown, 1967) and the Thingmuli lava series of Iceland (Carmichael, 1964). The dashed line represents a speculative liquid line of descent for a Kap Edvard Holm magma that begins crystallizing magnetite extensively at the apex of the curve, as a result of hydration or oxidation of the system.

Implications for the Kap Edvard Holm Complex and other mafic intrusions

Bernstein *et al.* (1992) proposed that gabbros of the Kap Edvard Holm Complex crystallized from dry tholeiitic magmas, on the basis of mineralogical similarities between Middle Layered Series gabbros and mid-ocean ridge basalts. In contrast, Wager & Brown (1967) proposed that the complex crystallized from magmas that were more oxidized

and more hydrous than typical tholeiites, on the basis of the relatively early appearance of cumulus magnetite and the widespread occurrence of interstitial amphibole and phlogopite. To reconcile these views, we propose that a compositional spectrum of magmas may have formed via the contamination of dry tholeiitic magmas by hydrous materials derived from the altered country rocks. The effects of contamination were apparently minor in the Lower and Middle Layered Series, but the cumulative effects of episodic contamination may account for distinctive mineralogical characteristics of the Upper Layered Series, the most evolved part of the complex. In the Upper Layered Series, cumulus magnetite is ubiquitous (Elsdon, 1971*a*), olivine is largely absent (Deer & Abbott, 1965; Elsdon, 1971*a*), and gabbroic pegmatites are abundant (Elsdon, 1971*a*). These features are similar to those of oxide gabbros at Stand and Deliver Nunatak, and might likewise be indicative of formation from hydrous contaminated magmas. This suggests that interaction with the hydrothermally altered country rocks may have affected the evolution of the entire complex in ways analogous to those proposed for postcumulus rocks in our study area.

The former existence of hydrous gabbroic magmas may also account for the existence, in the Kap Edvard Holm Complex and other layered intrusions, of laterally extensive ultramafic layers that are concordant over distances of hundreds of meters or a few kilometers, but which have discordant apophyses extending for centimeters or meters into layered cumulates above or below (e.g. Bernstein *et al.*, 1992, 1996; Tegner & Wilson, 1993; Tegner & Robins, 1996). Such layers in the Kap Edvard Holm Complex have previously been identified as ultramafic sills, some of which are postulated to have grown along their margins by metasomatic replacement of surrounding gabbroic cumulates (e.g. Bernstein *et al.*, 1992, 1996; Tegner & Wilson, 1993). In many cases, however, the extraordinary lateral continuity along strike and the close similarity of mineral compositions in ultramafic rocks and surrounding layered gabbros (Bernstein *et al.*, 1992, 1996; Tegner & Wilson, 1993; Arnason, 1995) seem more easily explicable if the ultramafic rocks are considered to be integral parts of the layered cumulus sequence rather than unrelated bodies of magma. Such an origin for many of the large ultramafic sheets would imply episodic influxes of hydrous magma or dehydration of country rocks during occasional stoping events, both of which are consistent with the open-system behavior of most large mafic magma systems.

CONCLUSION

From a combination of field, mineralogical, and geochemical evidence, we conclude that the ultramafic and oxide gabbro bodies at Stand and Deliver Nunatak formed from anomalously hydrous magmas, some of which may have been more oxidized than the main body of gabbro. At small scales, swarms of postcumulus bodies formed around xenoliths of metabasalt in response to *in situ* contamination of the host magma by hydrous fluids or melts that were expelled from the xenoliths. At larger scales, thick layers or sheets of ultramafic rock and oxide gabbro formed from magmas that were similarly contaminated within the magma chamber or during transit through the hydrothermally altered crust. Contamination resulting from devolatilization or partial assimilation of country rocks is thus inferred to have shifted phase relationships in the crystallizing magma, creating a variety of rock types and potentially altering liquid lines of descent in the evolving pluton. This mechanism of contamination could potentially influence magmatic evolution in a great variety of geologic environments in which mafic magmas are emplaced into hydrothermally altered basaltic crust.

ACKNOWLEDGEMENTS

We thank John Arnason, Stefan Bernstein, C. Kent Brooks, Peter Keleman, Richard Nevle, Peggy O'Day, Geoff Radford, Hreinn Skagfjord, and Christian Tegner for their help in the field and for stimulating geological discussions. Platinova Resources Ltd and Dihedral Exploration provided valuable logistical support. Rónadh Cox, Tamara Lowe and Joel Sparks helped with the XRF analyses, Robert Cullers and his staff conducted the INAA, and James Wright and his staff conducted the Sr isotope analyses. Peter Schiffman and Sarah Roeske provided valuable assistance at the UC Davis electron microprobe facility. Insightful reviews were provided by Stefan Bernstein, Alan Boudreau and Richard Wilson, and thoughtful comments on an early version of the manuscript were provided by Thrainn Fridriksson, Phil Neuhoff and Troels Nielsen. The work presented here is based largely on a Ph.D. thesis written by the first author while at Stanford University, and revisions were made while D.K.B. was on sabbatical leave at the Danish Lithosphere Center. Financial support was provided by the National Science Foundation (Grants NSF-EAR-8803754, NSF-EAR-9004007, NSF-EAR-9220431 and NSF-EAR-9506469, all to D.K.B.), the Richard and Frances Jahns Fund, the Geological Society of America, the Chevron Corporation, the Shell Corporation, and the McGee Trust.

REFERENCES

Abbott, D. & Deer, W. A. (1972). Geological investigations in East Greenland, Part X: the gabbro cumulates of the Kap Edvard Holm Lower Layered Series. *Meddelelser om Grønland* **190,** 1–42.

Andersen, D. J., Lindsley, D. H. & Davidson, P. M. (1993). QUILF: a PASCAL program to assess equilibria among Fe–Mg–Ti oxides, pyroxenes, olivine, and quartz. *Computers in Geosciences* **19,** 1333–1350.

Arnason, J. G. (1995). Gold and platinum-group mineralization in Tertiary mafic intrusions of East Greenland. Ph.D. Dissertation, Stanford University, CA.

Beard, J. S. & Lofgren, G. E. (1991). Dehydration melting and water-saturated melting of basaltic and andesitic greenstones and amphibolites at 1, 3, and 6·9 kbar. *Journal of Petrology* **32,** 365–401.

Bédard, J. H. & Hébert, R. (1996). The lower crust of the Bay of Islands ophiolite, Canada: petrology, mineralogy, and the importance of syntexis in magmatic differentiation in ophiolites and at ocean ridges. *Journal of Geophysical Research* **101,** 25105–25124.

Bédard, J. H., Sparks, R. S. J., Renner, R., Cheadle, M. J. & Hallworth, M. A. (1988). Peridotite sills and metasomatic gabbros in the Eastern Layered Series of the Rhum complex. *Journal of the Geological Society, London* **145,** 207–224.

Bernstein, S., Rosing, M. T., Brooks, C. K. & Bird, D. K. (1992). An ocean-ridge type magma chamber at a passive volcanic, continental margin: the Kap Edvard Holm layered gabbro complex, East Greenland. *Geological Magazine* **129,** 437–456.

Bernstein, S., Keleman, P. B. & Brooks, C. K. (1996). Evolution of the Kap Edvard Holm Complex: a mafic intrusion at a rifted continental margin. *Journal of Petrology* **37,** 497–519.

Bird, D. K., Rosing, M. T., Manning, C. E. & Rose, N. M. (1985). Geologic field studies of the Miki Fjord Area, East Greenland. *Bulletin of the Geological Society of Denmark* **34,** 219–235.

Bird, D. K., Manning, C. E. & Rose, N. M. (1988). Hydrothermal alteration of Tertiary layered gabbros, East Greenland. *American Journal of Science* **288,** 405–457.

Bird, D. K., Arnason, J. G., Brandriss, M. E., Nevle, R. J., Radford, G., Bernstein, S., Gannicott, R. A. & Kelemen, P. B. (1995). A gold-bearing horizon in the Kap Edvard Holm Complex, East Greenland. *Economic Geology* **90,** 1288–1300.

Boudreau, A. E. (1988). Investigations of the Stillwater Complex: Part IV. The role of volatiles in the petrogenesis of the J-M reef, Minneapolis adit section. *Canadian Mineralogist* **26,** 193–208.

Boudreau, A. E. (1999). Fluid fluxing of cumulates: the J-M reef and associated rocks of the Stillwater Complex, Montana. *Journal of Petrology* **40,** 755–772.

Brandriss, M. E. (1993). Assimilation of metabasalt xenoliths and postcumulus metasomatism of gabbros in the Kap Edvard Holm Complex, East Greenland. Ph.D. Dissertation, Stanford University, CA.

Brandriss, M. E., Nevle, R. J., Bird, D. K. & O'Neil, J. R. (1995). Imprint of meteoric water on the stable isotope compositions of igneous and secondary minerals, Kap Edvard Holm Complex, East Greenland. *Contributions to Mineralogy and Petrology* **121,** 74–86.

Brandriss, M. E., Bird, D. K., O'Neil, J. R. & Cullers, R. L. (1996). Dehydration, partial melting and assimilation of metabasaltic xenoliths in gabbros of the Kap Edvard Holm Complex, East Greenland. *American Journal of Science* **296,** 333–393.

Butcher, A. R. (1985). Channelled metasomatism in Rhum layered cumulates—evidence from late-stage veins. *Geological Magazine* **122,** 503–518.

Butcher, A. R., Young, I. M. & Faithfull, J. W. (1985). Finger structures in the Rhum Complex. *Geological Magazine* **122,** 491–502.

Carmichael, I. S. E. (1964). The petrology of Thingmuli, a Tertiary volcano in East Greenland. *Journal of Petrology* **5,** 435–460.

Carmichael, I. S. E. & Ghiorso, M. S. (1986). Oxidation–reduction relations in basic magma: a case for homogeneous equilibria. *Earth and Planetary Science Letters* **78,** 200–210.

Cullers, R., Chaudhuri, S., Kilbane, N. & Koch, R. (1979). Rare-earths in size fractions and sedimentary rocks of Pennsylvanian–Permian age from the mid-continent of the U.S.A. *Geochimica et Cosmochimica Acta* **43,** 1285–1301.

Davidson, J. P. & Tepley, F. J. III (1997). Recharge in volcanic systems: evidence from isotope profiles of phenocrysts. *Science* **275,** 826–829.

Davidson, P. M. & Lindsley, D. H. (1989). Thermodynamic analysis of pyroxene–olivine–quartz equilibria in the system CaO–MgO–FeO–SiO_2. *American Mineralogist* **74,** 18–30.

Deer, W. A. & Abbott, D. (1965). Clinopyroxenes of the gabbro cumulates of the Kap Edvard Holm complex, East Greenland. *Mineralogical Magazine*, Tilley volume, 177–193.

Dick, H. J. B., Meyer, P. S., Bloomer, S., Kirby, S., Stakes, D. & Mawer, C. (1991). Lithostratigraphic evolution of an *in situ* section of oceanic layer 3. In: Von Herzen, R. P., Robinson, P. T., *et al.* (eds) *Proceedings of the Ocean Drilling Program, Scientific Results, 118*. College Station, TX: Ocean Drilling Program, pp. 439–538.

Elsdon, R. (1969). The structure and intrusive mechanism of the Kap Edvard Holm layered gabbro complex, East Greenland. *Geological Magazine* **106,** 46–56.

Elsdon, R. (1971*a*). Crystallization history of the Upper Layered Series, Kap Edvard Holm, East Greenland. *Journal of Petrology* **12,** 499–521.

Elsdon, R. (1971*b*). Clinopyroxenes from the Upper Layered Series, Kap Edvard Holm Complex, East Greenland. *Mineralogical Magazine* **38,** 49–57.

Emeleus, C. H. (1987). The Rhum layered complex, Inner Hebrides, Scotland. In: Parsons, I. (ed.) *Origins of Igneous Layering*. Dordrecht: D. Reidel, pp. 263–286.

Fehlhaber, K. & Bird, D. K. (1991). Oxygen-isotope exchange and mineral alteration in gabbros of the Lower Layered Series, Kap Edvard Holm Complex, East Greenland. *Geology* **19,** 819–822.

Fram, M. S. & Lesher, C. E. (1997). Generation and polybaric differentiation of East Greenland early Tertiary flood basalts. *Journal of Petrology* **38,** 231–275.

Frost, B. R. & Lindsley, D. H. (1992). Equilibria among Fe–Ti oxides, pyroxenes, olivine, and quartz: Part II. Application. *American Mineralogist* **77,** 1004–1020.

Gaetani, G. A., Grove, T. L. & Bryan, W. B. (1994). Experimental phase relations of basaltic andesite from Hole 839B under hydrous and anhydrous conditions. In: Hawkins, J., Parsons, L., Allan, J., *et al.* (eds) *Proceedings of the Ocean Drilling Program, Scientific Results, 135*. College Station, TX: Ocean Drilling Program, pp. 557–563.

Ghiorso, M. S. (1997). Thermodynamic models of igneous processes. *Annual Review of Earth and Planetary Sciences* **25,** 221–241.

Ghiorso, M. S. & Carmichael, I. S. E. (1985). Chemical mass transfer in magmatic processes, II: Applications in equilibrium crystallization, fractionation and assimilation. *Contributions to Mineralogy and Petrology* **90,** 121–141.

Ghiorso, M. S. & Sack, R. O. (1995). Chemical mass transfer in magmatic processes IV. A revised and internally consistent thermodynamic model for the interpolation and extrapolation of liquid–solid equilibria in magmatic systems at elevated temperatures and pressures. *Contributions to Mineralogy and Petrology* **119,** 197–212.

Gordon, G. E., Randle, K., Goles, G., Corliss, J., Beeson, M. H. & Olsey, S. S. (1968). Instrumental neutron activation analysis of standard rocks with high-resolution gamma ray detectors. *Geochimica et Cosmochimica Acta* **32,** 369–396.

Helz, R. T. (1976). Phase relations of basalts in their melting ranges at P_{H2O} = 5 kb. Part II. Melt compositions. *Journal of Petrology* **17,** 139–193.

Helz, R. T. (1987). Differentiation behavior of Kilauea Iki lava lake, Kilauea Volcano, Hawaii: an overview of past and current work.

In: Mysen, B. O. (ed.) *Magmatic Processes: Physicochemical Principles*. San Antonio, TX: The Geochemical Society, pp. 241–258.

Hofmann, A. (1972). Chromatographic theory of infiltration metasomatism and its application to feldspars. *American Journal of Science* **272,** 69–90.

Holloway, J. R. & Burnham, C. W. (1972). Melting relations of basalt with equilibrium water pressure less than total pressure. *Journal of Petrology* **13,** 1–29.

Holm, P. M. (1988). Nd, Sr and Pb isotope geochemistry of the Lower Lavas, E Greenland Tertiary Igneous Province. In: Morton, A. C. & Parsons, L. M. (eds) *Early Tertiary Volcanism and the Opening of the NE Atlantic. Geological Society, London, Special Publication* **39,** 181–195.

Hunter, R. H. (1987). Textural equilibrium in layered igneous rocks. In: Parsons, I. (ed.) *Origins of Igneous Layering*. Dordrecht: D. Reidel, pp. 473–503.

Huppert, H. E. & Sparks, R. S. J. (1980). The fluid dynamics of a basaltic magma chamber replenished by influx of hot, dense ultrabasic magma. *Contributions to Mineralogy and Petrology* **75,** 279–289.

Irvine, T. N. (1987). Layering and related structures in the Duke Island and Skaergaard intrusions: similarities, differences, and origins. In: Parsons, I. (ed.) *Origins of Igneous Layering*. Dordrecht: D. Reidel, pp. 185–245.

Jacobs, J. W., Korotov, R. L., Blanchard, D. P. & Haskin, L. A. (1977). A well-tested procedure for instrumental neutron activation analysis of silicate rocks and minerals. *Journal of Radioanalytical Chemistry* **40,** 93–114.

Juster, T. C., Grove, T. L. & Perfit, M. R. (1989). Experimental constraints on the generation of FeTi basalts, andesites, and rhyodacites at the Galapagos Spreading Center, 85°W and 95°W. *Journal of Geophysical Research* **94,** 9251–9274.

Juteau, T., Ernewein, M., Reuber, I., Whitechurch, H. & Dahl, R. (1988). Duality of magmatism in the plutonic sequence of the Sumail Nappe, Oman. *Tectonophysics* **151,** 107–135.

Kays, M. A., Goles, G. G. & Grover, T. W. (1989). The Precambrian sequence bordering the Skaergaard intrusion. *Journal of Petrology* **30,** 321–361.

Korzhinskii, D. S. (1965). The theory of systems with perfectly mobile components and processes of mineral formation. *American Journal of Science* **263,** 193–205.

Korzhinskii, D. S. (1970). *Theory of Metasomatic Zoning*. Oxford: Clarendon Press.

Larsen, R. B. & Brooks, C. K. (1994). Origin and evolution of gabbroic pegmatites in the Skaergaard Intrusion, East Greenland. *Journal of Petrology* **35,** 1651–1679.

Laurent, R., Dion, C. & Thibault, Y. (1991). Structural and petrological features of peridotite intrusions from the Troodos Ophiolite, Cyprus. In: Peters, T., Nicolas, A. & Coleman, R. J. (eds) *Ophiolite Genesis and Evolution of the Oceanic Lithosphere*. Dordrecht: Kluwer Academic, pp. 175–194.

Lindsley, D. H. & Frost, B. R. (1992). Equilibria among Fe–Ti oxides, pyroxenes, olivine, and quartz: Part I. Theory. *American Mineralogist* **77,** 987–1003.

Mathez, E. A. (1984). Influence of degassing on oxidation states of basaltic magmas. *Nature* **310,** 371–375.

Mathez, E. A. (1989). Vapor associated with mafic magma and controls on its composition. In: Whitney, J. A. & Naldrett, A. J. (eds) *Ore Deposition Associated with Magmas*. El Paso, TX: Society of Economic Geologists, pp. 21–31.

Mathez, E. A. (1995). Magmatic metasomatism and formation of the Merensky reef, Bushveld Complex. *Contributions to Mineralogy and Petrology* **119,** 277–286.

McBirney, A. R. & Sonnenthal, E. L. (1990). Metasomatic replacement in the Skaergaard Intrusion, East Greenland: preliminary observations. *Chemical Geology* **88,** 245–260.

Meurer, W. P., Klaber, S. & Boudreau, A. E. (1997). Discordant bodies from olivine-bearing zones III and IV of the Stillwater Complex, Montana—evidence for postcumulus fluid migration and reaction in layered intrusions. *Contributions to Mineralogy and Petrology* **130,** 81–92.

Mitchell, A. A., Naicker, S. B., Marsh, J. S. & Dunlevey, J. N. (1997). The petrology and significance of a stratiform mafic segregation pegmatite in a Karoo-aged dolerite sheet. *South African Journal of Geology* **100,** 251–260.

Morse, S. A., Owens, B. E. & Butcher, A. R. (1987). Origin of finger structures in the Rhum complex: phase equilibrium and heat effects. *Geological Magazine* **124,** 205–210.

Natland, J. H., Meyer, P. S., Dick, H. J. B. & Bloomer, S. H. (1991). Magmatic oxides and sulfides in gabbroic rocks from Hole 735B and the later development of the liquid line of descent. In: Von Herzen, R. P., Robinson, P. T., *et al.* (eds) *Proceedings of the Ocean Drilling Program, Scientific Results, 118*. College Station, TX: Ocean Drilling Program, pp. 75–111.

Nevle, R. J., Brandriss, M. E., Bird, D. K., McWilliams, M. O. & O'Neil, J. R. (1994). Tertiary plutons monitor climate change in East Greenland. *Geology* **22,** 775–778.

Nielsen, T. F. D., Soper, N. J., Brooks, C. K., Faller, A. M., Higgins, A. C. & Matthews, D. W. (1981). The pre-basaltic sediments and the Lower Basalts at Kangerdlugssuaq, East Greenland: their stratigraphy, lithology, palaeomagnetism and petrology. *Meddelelser om Grønland, Geoscience* **6,** 1–25.

Norrish, K. & Chappell, B. W. (1977). X-ray fluorescence spectrometry. In: Zussmann, J. (ed.) *Physical Methods in Determinative Mineralogy*. New York: Academic Press, pp. 201–272.

Norrish, K. & Hutton, J. T. (1969). An accurate X-ray spectrographic method for the analysis of a wide range of geological samples. *Geochimica et Cosmochimica Acta* **33,** 431–453.

Norton, D. L. & Knapp, R. B. (1977). Transport phenomena in hydrothermal systems: the nature of porosity. *American Journal of Science* **277,** 913–936.

Osborn, E. F. (1959). Role of oxygen pressure in the crystallization and differentiation of basaltic magma. *American Journal of Science* **257,** 609–647.

Pankhurst, R. J., Beckinsale, R. D. & Brooks, C. K. (1976). Strontium and oxygen isotopic evidence relating to the petrogenesis of the Kangerdlugssuaq alkaline intrusion, East Greenland. *Contributions to Mineralogy and Petrology* **54,** 17–42.

Puffer, J. H. & Horter, D. L. (1993). Origin of pegmatitic segregation veins within flood basalts. *Geological Society of America Bulletin* **105,** 738–748.

Robins, B. (1982). Finger structures in the Lille Kufjord layered intrusion, Finnmark, northern Norway. *Contributions to Mineralogy and Petrology* **81,** 290–295.

Robins, B., Haukvik, L. & Jansen, S. (1987). The organization and internal structure of cyclic units in the Honningsvåg intrusive suite, North Norway: implications for intrusive mechanisms, double-diffusive convection and pore–magma infiltration. In: Parsons, I. (ed.) *Origins of Igneous Layering*. Dordrecht: D. Reidel, pp. 287–312.

Sato, M. (1978). Oxygen fugacity of basaltic magmas and the role of gas-forming elements. *Geophysical Research Letters* **5,** 447–449.

Scoon, R. N. & Mitchell, A. A. (1994). Discordant iron-rich ultramafic pegmatites in the Bushveld Complex and their relationship to iron-rich intercumulus and residual liquids. *Journal of Petrology* **35,** 881–917.

Sisson, T. W. & Grove, T. L. (1993). Experimental investigations of the role of H_2O in calc-alkaline differentiation and subduction zone magmatism. *Contributions to Mineralogy and Petrology* **113,** 143–166.

Sonnenthal, E. L. & McBirney, A. R. (1998). The Skaergaard layered series, part IV. Reaction-transport simulations of foundered blocks. *Journal of Petrology* **39,** 633–661.

Spulber, S. D. & Rutherford, M. J. (1983). The origin of rhyolite and plagiogranite in oceanic crust: an experimental study. *Journal of Petrology* **24,** 1–25.

Stewart, B. W. & DePaolo, D. J. (1990). Isotopic studies of processes in mafic magma chambers: II. The Skaergaard intrusion, East Greenland. *Contributions to Mineralogy and Petrology* **104,** 125–141.

Tegner, C. & Robins, B. (1996). Picrite sills and crystal–melt reactions in the Honningsvåg Intrusive Suite, northern Norway. *Mineralogical Magazine* **60,** 53–66.

Tegner, C. & Wilson, J. R. (1993). A late ultramafic suite in the Kap Edvard Holm layered gabbro complex, East Greenland. *Geological Magazine* **130,** 431–442.

Tegner, C., Wilson, J. R. & Brooks, C. K. (1993). Intraplutonic quench zones in the Kap Edvard Holm Layered Gabbro Complex, East Greenland. *Journal of Petrology* **34,** 681–710.

Tegner, C., Duncan, R. A., Bernstein, S., Brooks, C. K., Bird, D. K. & Storey, M. (1998). ^{40}Ar–^{39}Ar geochronology of Tertiary mafic intrusions along the East Greenland rifted margin; relation to flood basalts and the Iceland hotspot track. *Earth and Planetary Science Letters* **156,** 75–88.

Toplis, M. J. & Carroll, M. R. (1995). An experimental study of the influence of oxygen fugacity on Fe–Ti oxide stability, phase relations, and mineral–melt equilibria in ferro-basaltic systems. *Journal of Petrology* **36,** 1137–1170.

Wager, L. R. & Brown, G. M. (1967). *Layered Igneous Rocks*. San Francisco, CA: W. H. Freeman.

Wager, L. R. & Deer, W. A. (1939). Geological investigations in East Greenland, Part III. The petrology of the Skaergaard intrusion, Kangerdlugssuaq, East Greenland. *Meddelelser om Grønland* **105,** 1–352.

Yoder, H. S. & Tilley, C. E. (1962). Origin of basalt magmas; an experimental study of natural and synthetic rock systems. *Journal of Petrology* **3,** 342–532.